

AAE 5626: Orbital Mechanics for Engineers

Mrinal Kumar[©]

October 15, 2022

Orbital Maneuvers

1 Types of Orbits

This is a non-exhaustive enumeration! We are only concerned with some of the most common orbit classifications, namely those based on altitude and inclination.

Classification based on altitude

1. Low Earth Orbits (LEO): Typically, satellites operating in altitudes between 150 km and 1000 km altitudes are said to be in *low Earth orbit*. Keep in mind that these numbers are used roughly and are not set in stone.
 - One of the biggest factors in LEO is atmospheric drag. However, the drag experienced by spacecraft in LEO is computed in a very different manner than “traditional” drag, say for aircraft. Recall that the underlying theory for the traditional $D = qSC_D$ relationship is the Navier Stokes equation. Also recall that the Navier Stokes equation is very general and is built upon the validity of only one assumption - that the flow is a *continuum*, i.e. the density is high enough to treat the fluid particles as a *continuous medium*. This is a fairly good approximation for altitudes up to about 80 km, below which aerodynamic forces (e.g. drag) and moments can be computed by integrating the pressure distribution obtained by solving the Navier Stokes equation.
 - The continuum assumption starts to break down in altitudes higher than 80 km as the atmosphere becomes more and more *rarified*. Beyond 120 km, it is extremely rarified and the “flow” seen by spacecraft is more like a bombardment by ensembles of air molecules. Consequently, the Navier Stokes equation can no longer be applied. This type of flow is called *free-molecular flow*. Of course, lift and drag are still present, but must now be computed using methods of statistical analysis.
 - For altitudes between 80 km and 120 km, the flow is called *transition flow*, and has characteristics “in-between” the continuum and free-molecular flows. The theory is not developed for this regime and empirical relationships (sometimes called bridging functions) are used to compute aerodynamic forces and moments.
 - Beyond 300 km, the atmosphere can be safely ignored.
 - The above classification of the atmosphere is based on the so-called Knudsen number (Kn) defined as

$$Kn = \frac{\lambda}{d} = \frac{\text{mean free path length of air molecules}}{\text{characteristic length of craft}} \quad (1)$$

- Clearly for continuum flow (tightly packed molecules \Rightarrow small free path length between collisions), Kn is small and increases as the atmosphere becomes increasingly rarified. As seen from Eq.(1), the “rarified-ness” of the atmosphere is a tussle between the average distance traversed by air

Altitude (km)	Knudsen Number	Flow Type	Drag Computation
$h \leq 80$	$Kn < 0.01$	Continuum	Navier Stokes equations
$80 < h \leq 120$	$0.01 < Kn \leq 10$	Transition	Empirical relations
$120 < h \leq 300$	$10 < Kn$	Free molecular	Statistical analysis
$300 < h$	—	No atmosphere	Drag = 0

Table 1: Atmosphere Classification and Drag Calculation

molecules between collisions and the average size of the spacecraft. Table (1) summarizes this discussion. From this table, we see that for LEO, $Kn > 10$ and drag is a factor if at least for some time duration, the spacecraft comes within 300 km of the Earth's surface.

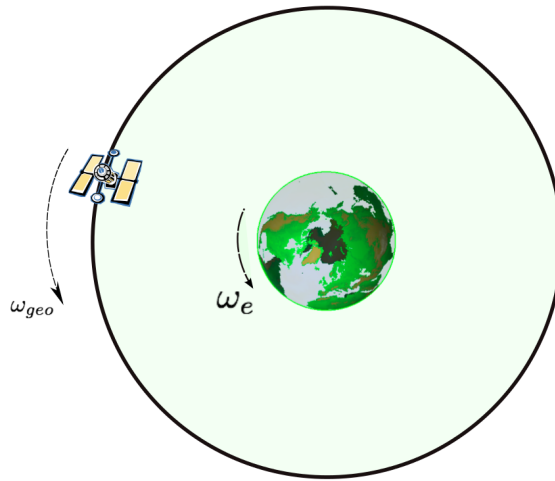
- Spacecraft in LEO are also well below the hazardous Van-Allen radiation belts. Van-Allen belts contain electrically charged particles that can damage sensitive equipment on-board. Roughly speaking, there are three layers of these belts and the inner-most layer exists between approximately 2400 km and 12,000 km altitude. The outermost Van-Allen belt lies approximately between 13,000 km and 60,000 km altitude.
- Typical types of spacecraft found in LEO: several manned spacecraft (e.g. the international space station), remote sensing satellites, imaging and navigation satellites. Typically, these spacecraft are in circular orbits.

2. High Earth Orbits (HEO): Anything greater than 1000 km altitude.

- Clearly, the atmosphere is not a factor for spacecraft in HEO. Van-Allen belts however do pose a threat and appropriate protection is needed.

3. Geostationary Equatorial Orbit (GEO): This is a special type of a HEO.

- GEO is very special because a spacecraft in it appears to be stationary to an observer on the Earth's surface. Clearly, this is possible only if the angular rate of the spacecraft is exactly the same as the rate of rotation of Earth. In terms of Fig.(1), this means $\omega_e = \omega_{geo}$.

Figure 1: Stationarity of a spacecraft in GEO: Top View. $\omega_e = \omega_{geo}$

- GEO is circular and has zero inclination (\sim equatorial orbit). To compute the speed of a spacecraft in GEO, we must first compute the rate of rotation of Earth. This is not as trivial as it sounds, because there are two types of “days”. The so-called *synodic day* is the typical day that goes from noon-to-noon and is 24 hours in duration. However, there is also a *sidereal day*, which is the time taken for Earth to complete one full rotation relative to the inertial reference frame attached to the stars. Essentially, this accounts for the discrepancy due to Earth’s motion around the Sun over one synodic day. Over one day, the Earth advances about $(2\pi/365.25)$ radians in its heliocentric orbit and this adds to the effective rotation about its axis. This is shown in an exaggerated manner in Fig.(2).

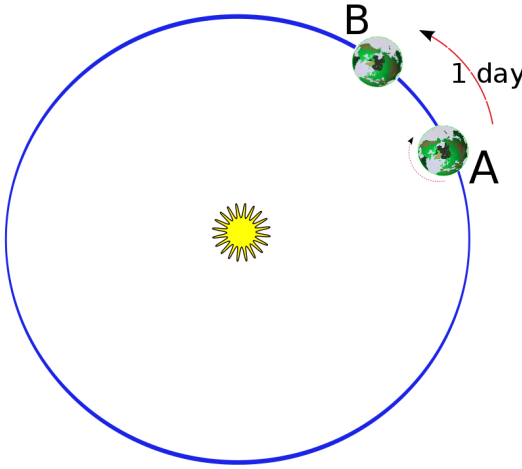


Figure 2: The sidereal day correction

- Thus, the inertial rotation rate of Earth is

$$\begin{aligned}\omega_e &= \frac{(2\pi + \frac{2\pi}{365.25})}{(24 \times 3600)} \text{ rad/s} \\ &= 7.29217 \times 10^{-5} \text{ rad/s}\end{aligned}\quad (2)$$

In order to be in GEO, the spacecraft must therefore must match this angular rate, i.e. $\omega_{geo} = \frac{v_{geo}}{r_{geo}} = \omega_e$. Or,

$$v_{geo} = \omega_e r_{geo} \quad (3)$$

Substitute this in the vis-viva equation and recall that GEO is circular to get

$$\omega_e^2 r_{geo}^2 = \frac{\mu}{r_{geo}} \quad (4)$$

which leads to the final result: $r_{geo} = (\mu/\omega_e^2)^{1/3}$. Eq.(3) gives us that $r_{geo} \approx 42164 \text{ km}$ (distance from Earth’s center).

- Communication and global-weather satellites are placed in GEO. Owing to its great altitude, GEO has high Earth coverage (at any time, it can view about 42% of the Earth’s surface). Of course, there is another benefit: constant tracking is not needed! (they are stationary when viewed from Earth).

Classification of orbits based on inclination

1. Equatorial orbits: These are orbits in the equatorial plane (i.e. their inclination is zero).

2. Polar orbits: These orbits have an inclination of 90 deg, i.e. they pass over the Earth's poles. It is expensive to place spacecraft in polar orbits (we will find out why).
3. Prograde orbits: Any orbit with inclination $0 \geq i \leq 90$ deg is called prograde. Essentially, an object in a prograde orbit moves in the same direction as the rotation of the central object, e.g. west to east for the Earth. All man-made geocentric spacecraft are in prograde orbits.
4. Retrograde orbits: An orbit with inclination $90 < i \leq 180$ deg is called retrograde. In this case, the object moves in a direction *opposite* to the direction of rotation of the central object. Retrograde orbits are rare and only certain natural objects like comets and certain moons are move in such orbits. Usually, these objects do not originate from the central object and are acquired by the mode of *capture*.
5. Molniya orbits: These are the Russian version on GEO. Since Russia does not have a low-latitude launch station, it is difficult for them to achieve equatorial orbits. Molniya orbits have very high inclination (≈ 60 deg) and are large and elliptical (periods > 12 hrs). Like the GEO satellites, they provide high coverage of the Earth.

2 Orbital Maneuvers

Quite often, it is required to move spacecraft from one orbit to another. For example, such maneuvers may be needed for rendezvous and docking of two spacecraft in separate orbits, to inject spacecraft into interplanetary trajectories, etc. The following are the basic assumptions of our study of orbital maneuvers:

- **A1:** *An orbit change will be achieved via a change in the velocity vector of the spacecraft.* I.E., if at a given point, the velocity vector of the spacecraft is changed (in magnitude, direction or both), it will leave its current orbit and start traveling in a new orbit. Alternatively, the orbit change will be affected via a so-called **DELTA-v**, or $\Delta\mathbf{v}$. In a sense, this is more of a *fact* than an assumption.

Fig.(3) presents an illustration. The orbit change takes place at point P , which is located at radius vector \mathbf{r} . The spacecraft is originally traveling on the orbit drawn with the solid-line. By application of the shown $\Delta\mathbf{v}$, the velocity vector changes, transferring the spacecraft onto the new orbit, drawn using a broken line.

Usually, the final orbit is known (it is the desired final destination). As a result, both \mathbf{v}_{old} and \mathbf{v}_{new} are known and it is just a matter of finding the required $\Delta\mathbf{v} = \mathbf{v}_{\text{new}} - \mathbf{v}_{\text{old}}$.

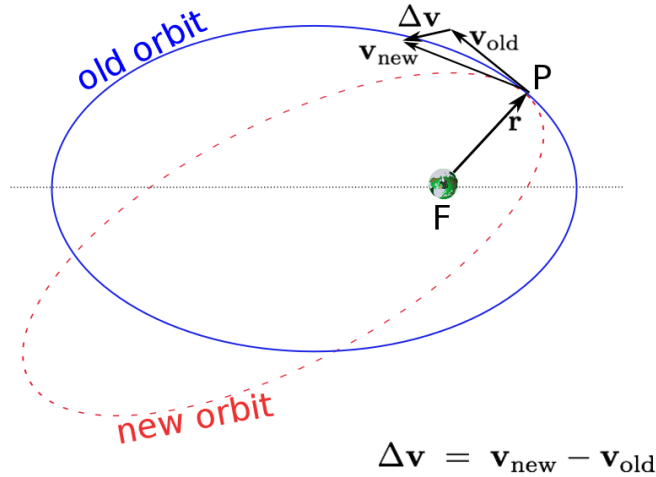
The point P can be called the “point of firing”. Note the following simple observation: the old and new orbits must share the point P ! Look at it another way, with the described method, it is only possible to transfer spacecraft between orbits that share at least one point in space.

- **A2:** *Velocity changes are instantaneous, or, impulsive.* Clearly, this is more of an assumption because any real rocket will take a finite amount of time to complete its burn, perhaps on the order of a few minutes. This is usually relatively small compared to the period of a typical orbit (on the order of hours) and thereby, impulsive $\Delta\mathbf{v}$ is a fairly accurate assumption. An exception: very low-thrust engines (e.g. modern ion engines) burn for very long durations and they must be treated separately.

The needed effort for an orbit change is not stated in terms of the amount of fuel required (Δm), but in terms of Δv (i.e. $\|\Delta\mathbf{v}\|$). Of course, Δm depends on Δv , but it also depends on the type of fuel used. An important descriptor of rocket fuels is the so-called “specific impulse”, I_{sp} . We have,

$$\frac{\Delta m}{m_0} = 1 - \exp\left(-\frac{\Delta v}{I_{sp}g}\right) \quad (5)$$

where, m_0 is the mass of the spacecraft before the start of the burn, Δm is the change in mass of the spacecraft due to the maneuver (i.e. the mass of propellant burned) and g is the acceleration due to gravity on Earth's surface, i.e. $g = 9.8 \text{ m/s}^2$, thus a constant. Table (2) presents a list of typical rocket fuels/thruster

Figure 3: Orbit changes via $\Delta\mathbf{v}$

Fuel/Thruster Type	I_{sp} (sec)	Comment
Mono-hydrazine	230	
Solid	290	
Nitric acid + Hydrazine	310	Typical
Liquid Oxygen + Hydrogen	455	Typical
Ion thruster	> 3000	very efficient but very slow (\Rightarrow non-impulsive)

Table 2: I_{sp} Values of Various Rocket Thrusters

types with their corresponding I_{sp} values. Usually, higher I_{sp} means a more efficient thruster but also a *slow burning* thruster (i.e. takes longer to complete the maneuver, affecting assumption **A2** above). The unit of I_{sp} is seconds.

3 Single Impulse Maneuvers

- Single impulse maneuvers are exactly what they sound like - they involve a single impulsive burn. Based on the discussion above, these maneuvers can only be executed between intersecting orbits. For example, consider Fig.(4). An initial orbit is shown and a final, desired orbit. It is desired to move the spacecraft from the former to the latter (perhaps it needs to dock with another spacecraft in the final orbit).

There are four points of intersection and they are all valid candidates for the location of executing the burn. Any of these four points will work, but, no other point will work! A very important question is, which point to choose as the point of firing? The simple answer is the following: keeping in mind that the final orbit is the same no matter what point is selected, pick the point that involves the minimum

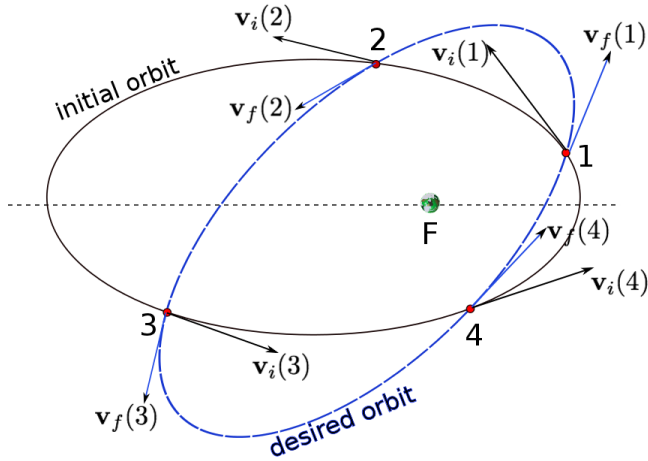


Figure 4: A General Single Impulse Scenario

Δv ! Note that

$$\begin{aligned}\Delta \mathbf{v}(1) &= \mathbf{v}_f(1) - \mathbf{v}_i(1) \\ \Delta \mathbf{v}(2) &= \mathbf{v}_f(2) - \mathbf{v}_i(2) \\ \Delta \mathbf{v}(3) &= \mathbf{v}_f(3) - \mathbf{v}_i(3) \\ \Delta \mathbf{v}(4) &= \mathbf{v}_f(4) - \mathbf{v}_i(4)\end{aligned}$$

Pick the firing point k at which $\Delta v(k) = \|\Delta \mathbf{v}(k)\|$ is the least. In case you are wondering, the RHS of each of the above equations is known since both the initial and final orbits are known.

- Suppose a single impulse maneuver is executed at a point with radius vector \mathbf{r} on a known initial orbit. In general, as a result of this maneuver, all the orbital elements will change:

$$\begin{aligned}\text{Initial: } (\mathbf{r}, \mathbf{v}_i) &\rightarrow (a, e, i, \omega, \Omega, f_0)_{\text{initial}} \\ \text{Final: } (\mathbf{r}, \mathbf{v}_f) &\rightarrow (a, e, i, \omega, \Omega, f_0)_{\text{final}}\end{aligned}$$

(The initial and final orbital parameters can be computed by walking through the integrals of motion.) Even though all parameters can be simultaneously changed, this is not how we will study orbital maneuvers here. Instead, we will look at ways to change one (or two) orbital parameters at a time. This approach is less efficient (leads to greater Δv), but is easier to analyze.

4 Single Impulse Maneuvers: Plane Change

The objective of a *single impulse plane change maneuver* is to change the orbital plane, i.e. inclination without disturbing other orbital elements. Recall our classification of orbital parameters:

$$\underbrace{a}_{\text{size}} \quad \underbrace{e}_{\text{shape}} \quad \underbrace{i, \omega, \Omega}_{\text{orientation}}$$

Therefore, the intention is to modify a single orientation parameter, namely inclination.

- Fig.(5) shows the geometry of a plane change maneuver. To ensure that the longitude of ascending node does not change, the maneuver must be executed at either the ascending (A) or descending (D) node. Based on the foregoing discussion, the ascending (and descending) nodes will be common between the initial and final orbits. Moreover, in order to ensure that the parameters a , e and ω do not change, the magnitude of \mathbf{v} , i.e. v must not be altered (why? - argue each one individually).
- Therefore, the velocity vector must only be purely rotated, such that *the orbital plane rotates with it*. Moreover, the axis of rotation is the line of nodes: See Fig.(5). Since $\|\mathbf{v}_i\| = \|\mathbf{v}_f\|$, does this mean

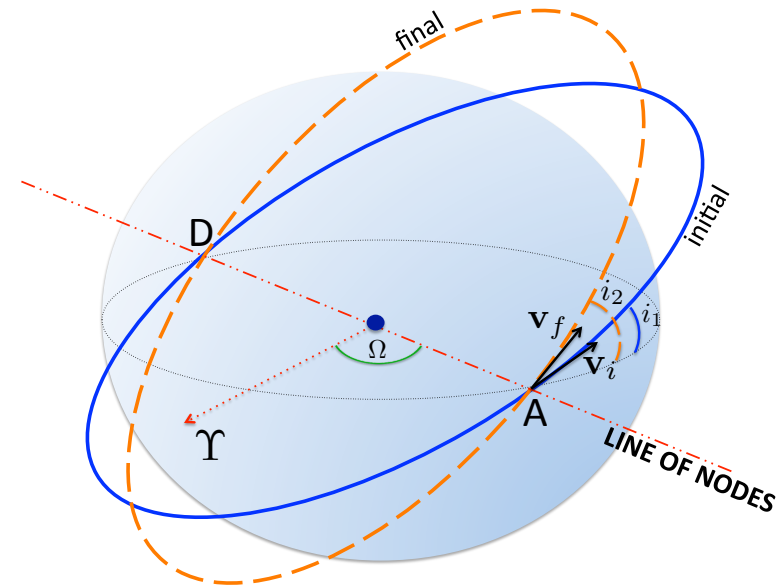


Figure 5: Single Impulse Plane Change Maneuver

$\Delta v = 0$? Of course not!

- Fig.(6) shows the geometry of the maneuver. The angle $\theta = (i_2 - i_1)$ is the change in inclination. Since $\|\mathbf{v}_i\| = \|\mathbf{v}_f\|$, the shown triangle is isosceles, from which we immediately get:

$$\frac{\Delta v}{2} = v \sin \frac{\theta}{2}, \text{ or,} \quad (6)$$

$$\Delta v = 2v \sin \frac{(i_2 - i_1)}{2} \quad (7)$$

All the Δv effort is used for a “mere re-orientation” of the velocity vector. Its magnitude remains the same! Note that the delta-v is directly proportional to the speed in orbit (v). Given that orbital speeds are fairly high, this implies that plane-change maneuvers are expensive! Also, can you argue that a plane change maneuver for LEO circular orbits will be significantly more expensive than plane changes for GEO?

• **Example** A spacecraft weighs 700 kg. Compute the Δv needed to achieve a plane change of 10 deg. The original orbit is circular of altitude 400 km. The fuel $I_{sp} = 300$ sec.

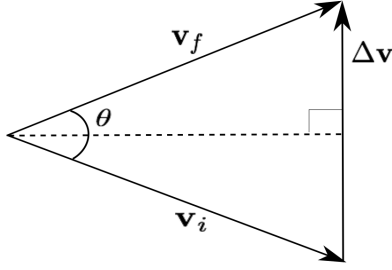


Figure 6: Geometry of the Plane Change Maneuver

Let us first determine the speed of spacecraft in its orbit:

$$v = \sqrt{\mu/r} = \sqrt{\frac{\mu}{R_e + 400 \times 10^3}} = 7.6686 \text{ kmps}$$

Therefore, using Eq.(7),

$$\Delta v = 2v \sin 5^\circ = 1.3367 \text{ kmps huge!}$$

Corresponding propellant mass:

$$\begin{aligned} \frac{\Delta m}{m_0} &= 1 - \exp\left(\frac{-\Delta v}{I_{sp}g}\right) \\ &= 0.3653; \end{aligned}$$

$$\text{i.e. } \Delta m = 0.3653 m_0 = 255.71 \text{ kg (propellant mass needed)}$$

Clearly, plane change is expensive!

- The following two exercises will provide further insight into the cost of plane change maneuvers.

- (A) Fig.(7) shows a circular orbit. A tangential velocity increment is provided at the shown firing point (P) so that the new orbit is parabolic. In other words, $\mathbf{v}_f = \mathbf{v}_{\text{escape}}$. Note that \mathbf{v}_i and \mathbf{v}_f are collinear, i.e. the entire $\Delta\mathbf{v}$ is used to increase the magnitude of the velocity vector. The question is simple: How much Δv is needed to accomplish the shown escape?

Since $\mathbf{v}_i \parallel \mathbf{v}_f$,

$$\Delta v = v_f - v_i \quad (8)$$

I.E., the $\Delta\mathbf{v}$ geometry reduces to a simple algebraic computation. We saw earlier that

$$v_f(r) = v_{\text{escape}}(r) = \sqrt{2}v_{\text{circular}}(r) = \sqrt{2}v_c(r) \quad (9a)$$

$$\text{And, } v_i(r) = v_{\text{circular}}(r) = v_c(r) \quad (9b)$$

Since $v_c(r) = \sqrt{\mu/r}$,

$$\Delta v_{\text{escape}} = (\sqrt{2} - 1)\sqrt{\frac{\mu}{r}} \quad (9c)$$

The next question is the following: suppose the above Δv was used not for escape, but for change of inclination; then how much of it is possible? Use the Δv from Eq.(9c) in Eq.(7) and find $\theta (= i_2 - i_1)$:

$$\Delta v_{\text{escape}} = (\sqrt{2} - 1)v_c = 2v_c \sin \frac{\theta}{2}$$

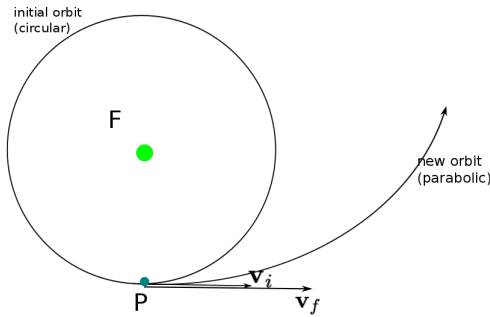


Figure 7: Escape from a circular orbit

$$\Rightarrow \theta = 2 \sin^{-1} \left(\frac{\sqrt{2} - 1}{2} \right) \approx 23.9 \text{ deg} \quad \text{wow!!} \quad (10)$$

The Δv that is sufficient to transfer a spacecraft from an initial circular orbit to an escape parabola, if applied to accomplish a pure inclination change, is good only for a mere 23.9 deg plane change! Incredibly, this number (23.9 deg) is independent of the altitude of the circular orbit (note that v_c cancels in Eq.(10)).

Moral of the story: plane changes are expensive!

(B) In the second exercise, simply set $\theta = 60$ deg in Eq.(7). The required Δv is

$$\Delta v(\theta = 60 \text{ deg}) = 2v \sin 30 = v$$

In other words, the required Δv for a 60 deg plane change equals 100% of the magnitude of the velocity vector, which is another indicator of the expense of plane changes. Corresponding propellant mass needed can be computed from Eq.(5):

$$\begin{aligned} \frac{\Delta m}{m_0} &= 1 - \exp \left(\frac{-\Delta v}{I_{sp}g} \right) \\ &= 0.926 \quad @ 400 \text{ km circular}, I_{sp} = 300s \end{aligned}$$

I.E., propellant mass needed to achieve a 60 deg plane change in a 400 km altitude circular orbit using a fuel with $I_{sp} = 300s$ is 92.6% of the spacecraft mass. Clearly, changing the orbital inclination is costly.

5 Single Impulse Maneuvers: Simultaneous Change in i and Ω

In the second type of single impulse maneuvers, we will consider simultaneously changing the inclination *and* the longitude of ascending node of the orbit.

- Recall that for a pure inclination change, the axis of rotation of the velocity vector was the line of nodes. This ensured that Ω did not change during the maneuver. Consider Fig.(8), in which the velocity vector is again purely rotated, but the axis of rotation is not the line of nodes. Similarly, the firing point is not at one of the nodes, and as a result, both i and Ω change.

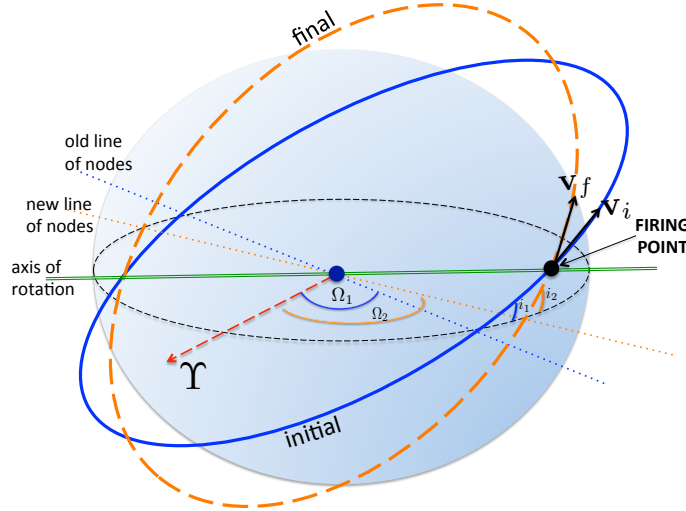
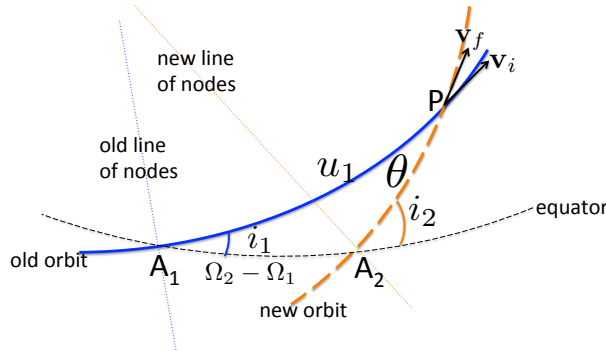


Figure 8: Simultaneous Change in Inclination and Longitude of Ascending Node

- Let the initial i and Ω be: i_1 and Ω_1 (both known). Similarly, let the final values be i_2 and Ω_2 , also known. The problem then is to find the angle “ θ ”, which is the angle by which the velocity vector must be rotated. Moreover, we also need to find the point of firing to achieve the desired orbit orientation. Both of these can be determined by solving the spherical triangle shown in Fig.(9). This triangle has been isolated from Fig.(8) and its vertices are: A_1 (ascending node of the initial orbit), A_2 (ascending node of the new orbit) and P (point of engine firing).

Figure 9: Geometry of a Composite Change in i and Ω

- In Fig.(9), u_1 is called the “argument of latitude or the firing point” and helps identify its location on the initial orbit, measured from the old ascending node A_1 to P , along the plane of the initial orbit. Recall the “argument of periapsis”: indeed, if the firing point turns out to be the same as the periapsis, $u_1 = \omega$. Also clearly shown in the figure is θ , which is the angle between the initial and final velocity vectors.

- Both u_1 and θ can be determined using the rules of spherical trigonometry for triangle A_1A_2P as follows:

$$\cos i_2 = \cos i_1 \cos \theta - \sin i_1 \sin \theta \cos u_1 \quad (11a)$$

$$\cos \theta = \cos i_1 \cos i_2 + \sin i_1 \sin i_2 \cos(\Omega_2 - \Omega_1) \quad (11b)$$

The unknown quantities are u_1 (location of P) and θ (required rotation of the velocity vector) and can be obtained by simultaneously solving the above two equations because all the other quantities are known. (Obtain θ first from Eq.(11b), then substitute in Eq.(11a) to get u_1)

- To finish, the maneuver is executed by rotating the vector \mathbf{v}_i by angle θ so that it coincides with \mathbf{v}_f . The magnitude of velocity remains unchanged, ensuring that no other orbital parameter is affected. The required Δv can be computed from Eq.(6). In this equation, please **do not** set $\theta = (i_2 - i_1)!$ Use the value of θ obtained from Eqs.(11) as described above.
- This maneuver has the same characteristics as a pure plane change (is directly proportional to v), and is therefore just as expensive.

6 Single Impulse Maneuvers: Apsidal Rotation

- An apsidal rotation rotates the line of apsides, i.e. the line connecting the periapsis and apoapsis. The rotation is performed in the plane of the orbit. The effect is a change in the orientation parameter ω without changing any other orbital parameter. Fig.(10) shows an illustration. $\Delta\omega$ is the angle by which the line of apses is rotated. There are two points of intersection between the initial and final orbits. Geometry of the velocity vectors at the lower intersection point (P_L) is shown.

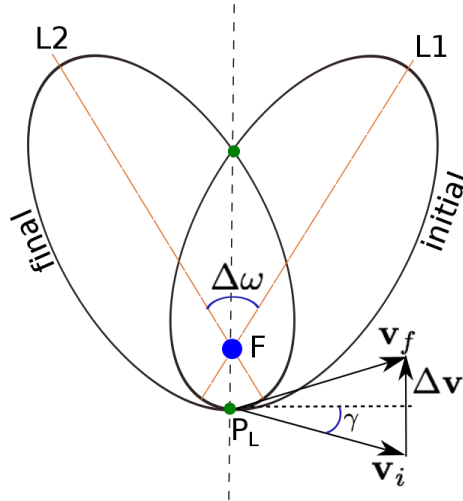


Figure 10: Geometry of an Apsidal Rotation.

- Owing to the pure rotation of the velocity vector, $v_f = v_i = v$ and the angle of rotation is 2γ . As we have seen multiple times thus far for a geometry like this, $\Delta v = 2v \sin \gamma$.
- The final step is to find the relationship between $\Delta\omega$ (known) and γ , allowing us to compute Δv .

Recall that $\gamma = \pi/2 - \angle(\mathbf{r}, \mathbf{v})$. Therefore,

$$h = \|\mathbf{r} \times \mathbf{v}\| = rv \sin\left(\frac{\pi}{2} - \gamma\right) = rv \cos \gamma \quad (12)$$

Using the equation of orbit ($r = p/(1 + e \cos f)$) in the vis-viva equation ($v^2/2 - \mu/r = -\mu/2a$), we get:

$$\begin{aligned} v^2 &= \mu \left(\frac{2(1 + e \cos f)}{p} - \frac{1}{a} \right) \\ &= \frac{\mu}{a} \left(\frac{2(1 + e \cos f)}{1 - e^2} - 1 \right) \\ &= v_c^2(p)(1 + e^2 + 2e \cos f) \end{aligned} \quad (13)$$

where, $v_c(p) = \sqrt{\mu/p}$ is the circular speed at $r = p$. Using the velocity found above, along with the parametric orbit equation in Eq.(12),

$$\begin{aligned} h^2 &= r^2 v^2 \cos^2 \gamma = \frac{p^2}{(1 + e \cos f)^2} v_c^2(p)(1 + e^2 + 2e \cos f) \cos^2 \gamma \\ &= \mu p \end{aligned} \quad (14)$$

Thus we get

$$\cos \gamma = \frac{1 + e \cos f}{\sqrt{1 + e^2 + 2e \cos f}} \quad \text{and,} \quad (15)$$

$$\sin \gamma = \frac{e \sin f}{\sqrt{1 + e^2 + 2e \cos f}} \quad (16)$$

Now consider an isolated view of the line of apsides shown in Fig.(11).

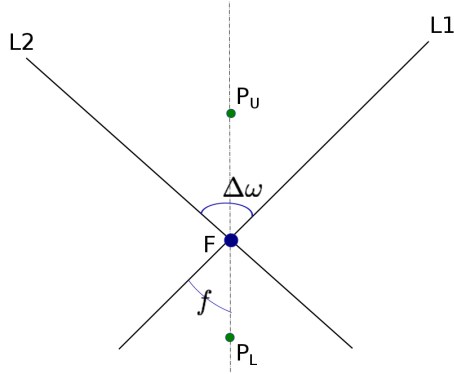


Figure 11: Isolated view of line of apsides.

The true anomalies of the two possible firing locations are:

$$f(P_L) = \frac{\Delta\omega}{2} \quad (17a)$$

$$f(P_U) = \pi + \frac{\Delta\omega}{2} \quad (17b)$$

Using Eqs.(17) in Eq.(16),

$$\sin \gamma_L = \frac{e \sin(\Delta\omega/2)}{\sqrt{1 + e^2 + 2e \cos(\Delta\omega/2)}} \quad (18a)$$

$$\sin \gamma_U = -\frac{e \sin(\Delta\omega/2)}{\sqrt{1 + e^2 - 2e \cos(\Delta\omega/2)}} \quad (18b)$$

To finish, use Eq.(13) and (18) in the expression for Δv to get:

$$\begin{aligned} (\Delta v)^2(P_L) &= 4v^2(P_L) \sin^2 \gamma_L \\ &= 4v_c^2(p)(1 + e^2 + 2e \cos f(P_L)) \frac{e^2 \sin^2(\Delta\omega/2)}{1 + e^2 + 2e \cos f(P_L)} \\ &= 4v_c^2(p)e^2 \sin^2(\Delta\omega/2) \end{aligned} \quad (19)$$

- The final result:

$$\frac{\Delta v(P_L)}{v_c(p)} = 2e \sin(\Delta\omega/2) \quad (20)$$

It is easy to show that $\Delta v(P_L) = \Delta v(P_U)$.

- It can be shown (we will not do this exercise here) that if the same apsidal rotation is accomplished via a *two-impulse maneuver* as opposed to a single impulse maneuver, the same orbit change can be achieved using only half the Δv obtained in Eq.(20). A schematic of this maneuver is shown in Fig.(12). This was shown in 1962 by Derek Lawden¹.

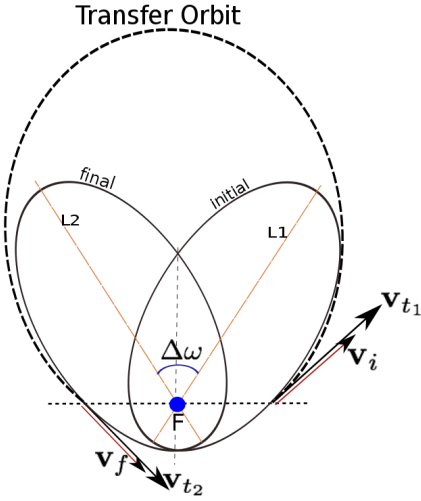


Figure 12: Two impulse rotation of the line of apsides.

In Fig.(12), the apsidal rotation is accomplished via a two-impulse maneuver, utilizing a so-called transfer orbit (we will see more of them soon). There are two *tangential* $\Delta \mathbf{v}$'s - maneuvers in which the initial and final velocity vectors are collinear, i.e. have the same direction. In such maneuvers, only the velocity magnitude (i.e. speed) changes - causing either a slow down or a speed up. Fig.(12) shows that the first maneuver involves a speed up, such that $\Delta v_1 = \|\mathbf{v}_{t_1} - \mathbf{v}_i\| = (v_{t_1} - v_i)$, and the

¹Lawden, D. F., "Impulsive Transfer Between Elliptical Orbits", *Optimization techniques, with applications to aerospace systems*, edited by G. Leitmann, Academic, New York, pp. 323-351: see attached in Carmen

second maneuver involves a slow-down, such that $\Delta v_2 = \|\mathbf{v}_{t_2} - \mathbf{v}_f\| = (v_{t_1} - v_i)$. Lawden showed that

$$\Delta v_1 = \Delta v_2 = \frac{e}{2} \sqrt{\frac{\mu}{p}} \sin(\Delta\omega/2) \quad (21)$$

Leading to a total $\Delta v = \Delta v_1 + \Delta v_2 = ev_c(p) \sin(\Delta\omega/2)$.

7 Single Impulse Maneuvers: Simultaneous Change in a and e

- In this single impulse maneuver, we will attempt a change only in the size (a) and shape (e) of orbit, without changing its orientation (i.e. i , Ω and ω).
- To illustrate this maneuver, let us assume that the initial orbit is circular: see Fig.(13). A tangential $\Delta\mathbf{v}$ is applied such that only the speed changes. This ensures that the orientation of the initial and final orbits remains the same. Since \mathbf{v}_i , \mathbf{v}_f and $\Delta\mathbf{v}$ are collinear, we have a simple algebraic equation:

$$\Delta v = v_f - v_i \quad (22)$$

Or, $v_f = v_i + \Delta v$.

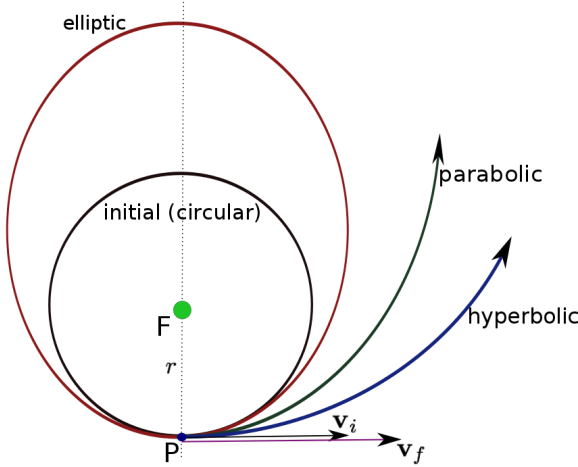


Figure 13: Change in size and shape of orbit.

- Note that in this example $v_f > v_i$, but this may not be true in general, i.e. the maneuver may involve a slow-down of the spacecraft. Therefore in general for tangential maneuvers, we write $\Delta v = |v_f - v_i|$.
- We will look at three cases as illustrated in Fig.(13). The point of firing (P) is shown.

I. Parabolic new orbit: such that $v_f = v_{\text{escape}}$. We have already encountered this case before:

$$v_i = v_c(r); \quad v_f = \sqrt{2}v_c(r) \quad (23)$$

such that

$$\Delta v = |v_f - v_i| = (\sqrt{2} - 1)v_c(r) = (\sqrt{2} - 1)\sqrt{\frac{\mu}{r}} \quad (24)$$

II. Elliptic new orbit: such that $v_i < v_f < v_{\text{escape}}$. In terms of Δv ,

$$0 < \Delta v < (\sqrt{2} - 1) \sqrt{\frac{\mu}{r}} \quad (25)$$

Using the vis-viva equation for the new orbit at point P,

$$\frac{v_f^2}{2} - \frac{\mu}{r} = -\frac{\mu}{2a} \quad (26)$$

but, $v_f^2 = (v_i + \Delta v)^2 = (v_c^2 + \Delta v^2 + 2v_c \Delta v)$. Using this in Eq.(26),

$$\frac{v_c^2}{2} + \frac{(\Delta v^2 + 2v_c \Delta v)}{2} - \frac{\mu}{r} = -\frac{\mu}{2a} \quad (27)$$

$$\Rightarrow a = \frac{-\mu}{(\Delta v^2 + 2v_c \Delta v - v_c^2)} \quad (28)$$

where, Δv is given in Eq.(25), and we have made use of the fact $v_c^2 = \mu/r$ in going from Eq.(27) to Eq.(28). Eq.(28) gives us the semi-major axis of the final orbit. If a is known, Eq.(28) must be solved to obtain the required Δv . Note this is a quadratic equation in Δv and it is easy to show that there exists a unique feasible answer.

The eccentricity can be found (if not already prescribed) using the relationship between a and radius of periapsis. It is easy to see from Fig.(13) that the point of firing is the periapsis of the new ellipse. Therefore, $r = r_p = a(1 - e)$, such that $e = (1 - r/a)$.

III. Hyperbolic new orbit: such that $v_f > v_{\text{escape}} > v_i$. In terms of Δv :

$$\Delta v > (\sqrt{2} - 1) \sqrt{\frac{\mu}{r}} \quad (29)$$

The semi-major axis and eccentricity for the new hyperbolic orbit can be found in the same manner as shown above for the ellipse.

8 Summary of Single Impulse Maneuvers

Table (3) summarizes the various single impulse maneuvers we encountered here.

Maneuver	Δv	Comments
Pure Δi	$\Delta v = 2v \sin \theta / 2$	$\theta = i_2 - i_1 = \Delta i$
Composite ($\Delta i, \Delta \Omega$)	$\Delta v = 2v \sin \theta / 2$	$\theta = \begin{cases} \Delta i \\ \Delta \Omega \end{cases}$
Pure $\Delta \omega$	$\Delta v = 2v_c(r = p)e \sin \Delta \omega / 2$	
Composite ($\Delta a, \Delta e$)	$0 < \Delta v < (\sqrt{2} - 1)v_c$	new orbit: ellipse
	$\Delta v = (\sqrt{2} - 1)v_c$	new orbit: parabola
	$\Delta v > (\sqrt{2} - 1)v_c$	new orbit: hyperbola

Table 3: Sumary of single impulse maneuvers

The first three rows of Table (3) represent pure rotations of the velocity vector without change in its magnitude. They are all very expensive. On the other hand, the fourth row requires tangential Δv , change

in only the magnitude of the velocity vector. In general, if it is possible to avoid rotation of the velocity vector by employing more than one impulse, the multi-impulse strategy must be adopted. An example of this was shown above in the section on apsidal rotation, in which the Δv requirement was cut in half by replacing a single pure rotation of the velocity vector by two tangential impulses. The final orbit in both cases was the same! So a valid question is, why would one ever go for the “more expensive maneuver”? The price to pay in exchange for a lower Δv is a more “time consuming maneuver”. This is however not a big problem, except in some extreme cases, e.g. when a rescue mission is involved.

9 Multi-Impulse Maneuvers

So far, we considered only single impulse maneuvers. Since maneuvers are assumed to be impulsive (i.e. instantaneous), single impulses can provide transfers *only* between intersecting orbits (i.e. orbits that share at least one common point in space). Of course, this constitutes only a very small portion of possible orbit maneuvers. The main lesson learned during our consideration of single impulse maneuvers was that pure rotations of the velocity vector are significantly more expensive than tangential Δv 's and must be avoided as much as possible. In this set of notes, we will consider multi-impulse maneuvers, thereby achieving more general orbital transfers.

10 Hohmann Transfers

The Hohmann transfer was originally designed for transfer between *co-planar circular orbits* and involves two impulses. It is the most fuel efficient maneuver possible between coplanar circular orbits. It is also the *slowest*, which is a price that must be paid for efficiency. Due to its leisurely nature, it is preferred for short transfers and/or when time is not a factor for mission health.

- Fig.(14) shows the geometry of a Hohmann transfer: the initial and final orbits are both circular with radii R_i and R_f respectively. They are connected by a “transfer ellipse” that essentially forms a bridge between them. The solid portion of the ellipse is traversed by the spacecraft whereas the dashed portion is never used.
- It is apparent from Fig.(14) that the Hohmann transfer involves two maneuvers (at points P and A) and both are tangential (a good thing!). There are three steps:
 - I. Design of the transfer ellipse (TE): Since the orbits are coplanar, this step is actually very easy. Let the semi-major axis of the transfer orbit be denoted by a_t . Then from Fig.(14),

$$2a_t = R_i + R_f \quad (30)$$

Moreover,

$$r_{p_t} = R_i \quad (\text{periapsis of TE}) \quad (31)$$

and,

$$r_{a_t} = R_f \quad (\text{apoapsis of TE}) \quad (32)$$

Therefore,

$$\frac{r_{a_t}}{r_{p_t}} = \frac{a_t(1+e_t)}{a_t(1-e_t)} = \frac{R_f}{R_i} \triangleq \chi \quad (33)$$

where χ is defined to be the ratio of the final radius to the initial radius. We can now solve for the eccentricity of TE (e_t):

$$e_t = \frac{\chi - 1}{\chi + 1} \quad (34)$$

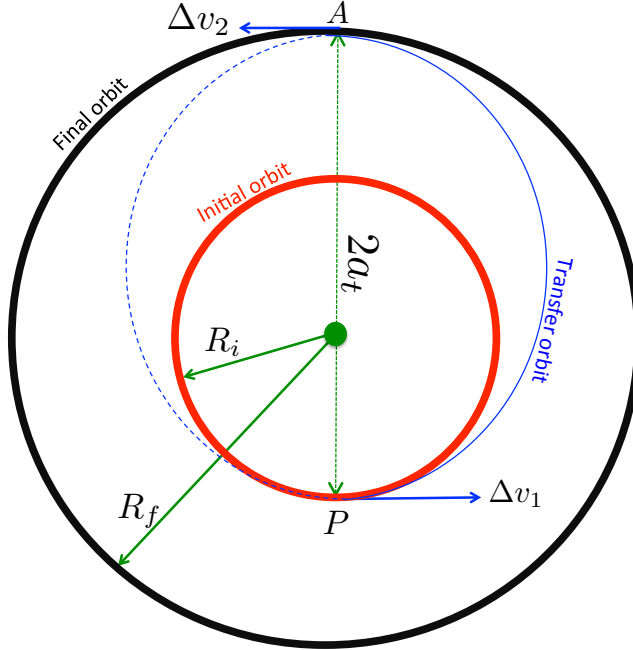


Figure 14: Geometry of the Hohmann Transfer

- II. Determine the magnitude of the first burn (@ P), i.e. Δv_1 : The speed on the initial orbit (being a circle) is simply

$$v_i = \sqrt{\frac{\mu}{R_i}} \quad (35)$$

Speed on TE @ P is the speed on TE at its periapsis, which can be found from the vis-viva equation for TE:

$$\frac{v_{p_t}^2}{2} - \frac{\mu}{R_i} = -\frac{\mu}{2a_t} \quad \left(r_{p_t} \underset{\text{Eq.(31)}}{=} R_i \right) \quad (36)$$

Using Eq.(30),

$$v_{p_t}^2 = 2\frac{\mu}{R_i} \left(1 - \frac{R_i}{R_i + R_f} \right) \quad (37a)$$

$$\underset{\text{Eqs.(33),(35)}}{=} 2v_i^2 \left(1 - \frac{1}{\chi + 1} \right) \quad (37b)$$

$$= 2v_i^2 \frac{\chi}{\chi + 1} \quad (37c)$$

Thus,

$$v_{p_t} = v_i \sqrt{\frac{2\chi}{\chi + 1}} \quad (38)$$

Since the burn is tangential, Δv_1 can simply be computed via an algebraic subtraction of v_i from v_{p_t} (as opposed to a vector subtraction), i.e. $\Delta v_1 = v_{p_t} - v_i$ (see Fig.(15)). Using Eqs.(38) and (35),

$$\boxed{\Delta v_1 = v_i \left(\sqrt{\frac{2\chi}{\chi + 1}} - 1 \right)} \quad (39)$$

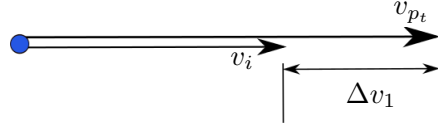


Figure 15: Geometry of the first burn in Hohmann transfer

III. Determine the magnitude of the second burn (@ A), i.e. Δv_2 : Since the final orbit is also circular, speed on it is simply

$$v_f = \sqrt{\frac{\mu}{R_f}} \quad (40)$$

Since point A is the apoapsis of the transfer ellipse, vis-viva gives us

$$v_{a_t}^2 = 2 \left(\frac{\mu}{R_f} - \frac{\mu}{R_i + R_f} \right) \quad (41a)$$

$$= 2 \frac{\mu}{R_i} \left(\frac{R_i}{R_f} - \frac{R_i}{R_i + R_f} \right) \quad (41b)$$

$$\stackrel{\text{Eqs.(35),(33)}}{=} 2v_i^2 \left(\frac{1}{\chi} - \frac{1}{\chi + 1} \right) \quad (41c)$$

$$= 2v_i^2 \frac{1}{\chi(\chi + 1)} \quad (41d)$$

Thus

$$v_a = v_i \sqrt{\frac{2}{\chi(\chi + 1)}} \quad (42)$$

Just like the maneuver at P, the maneuver at A is tangential (see Fig.(16) for geometry), and an algebraic subtraction gives

$$\Delta v_2 = v_f - v_{a_t} \quad (43a)$$

$$\stackrel{\text{Eqs.(40),(42)}}{=} \sqrt{\frac{\mu}{R_f}} - v_i \sqrt{\frac{2}{\chi(\chi + 1)}} \quad (43b)$$

$$= v_i \sqrt{\frac{1}{\chi}} - v_i \sqrt{\frac{2}{\chi(\chi + 1)}} \quad (43c)$$

Or,

$$\boxed{\Delta v_2 = \frac{v_i}{\sqrt{\chi}} \left(1 - \sqrt{\frac{2}{\chi + 1}} \right)} \quad (44)$$

Note that $v_f > v_{a_t}$ because the final orbit is bigger than the transfer ellipse (i.e. has a bigger semi-major axis and thus greater energy).

- To finish our analysis of the Hohmann transfer between coplanar circular orbits, we add the two- Δv 's to determine the *total* Δv needed (total effort):

$$\boxed{\Delta v_{\text{Hohmann}} = \Delta v_1 + \Delta v_2 = v_i \left[\sqrt{\frac{2\chi}{\chi + 1}} - 1 + \frac{1}{\sqrt{\chi}} \left(1 - \sqrt{\frac{2}{\chi + 1}} \right) \right]} \quad (45)$$

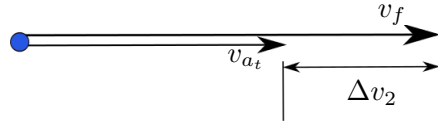


Figure 16: Geometry of the second burn in Hohmann transfer

- It is also important to compute the total time consumed in performing the transfer: note that the actual impulses consume zero time. However, the spacecraft must traverse half the TE (solid portion in Fig.(14)) in between the two burns. Since the traversal is from the periapsis to the apoapsis of the TE, the time consumed is half its period, i.e. $P_t/2$. Thus we have

$$\boxed{\text{Transfer time} = \pi \sqrt{\frac{a_t^3}{\mu}}} \quad (46)$$

- Note:** The above analysis of the Hohmann transfer assumed that the initial orbit is smaller than the final orbit. But it doesn't have to be! Can you argue that the maneuver will look *exactly* the same, with the same total Δv and the same time of execution if you swap the initial and final orbits? Just repeat the three-step procedure described above.

• **Example** Design the Hohmann transfer of a spacecraft of mass 700 kg between coplanar circular orbits of radii $R_f = 2R_i = 14,000$ km. Propellant efficiency: $I_{sp} = 250$ s.

We will do this step by step:

- Design of transfer ellipse: (see details above):

$$a_t = \frac{R_i + R_f}{2} = 10,500 \text{ km} \quad (47a)$$

$$e_t = \frac{\chi - 1}{\chi + 1} = 1/3 \quad (47b)$$

$$P_t = 2\pi \sqrt{\frac{a_t^3}{\mu}} = 2.974 \text{ hrs} \quad (47c)$$

- First Burn:

$$\Delta v_1 = v_i \left(\sqrt{\frac{2\chi}{\chi + 1}} - 1 \right) = \left(\frac{2}{\sqrt{3}} - 1 \right) v_i \quad (48)$$

where, $v_i = \sqrt{\mu/R_i} = 7.5461$ kmps. Thus, $\Delta v_1 = 1.1674$ kmps.

- Second Burn:

$$\Delta v_2 = \frac{v_i}{\sqrt{\chi}} \left(1 - \sqrt{\frac{2}{\chi + 1}} \right) = \frac{v_i}{\sqrt{2}} \left(1 - \sqrt{\frac{2}{3}} \right) = 979.15 \text{ m/s} \quad (49)$$

Thus we get:

- Total $\Delta v = \Delta v_1 + \Delta v_2 = 2.1465$ kmps.
- Time to completion: $T = P_t/2 = 1.487$ hr ≈ 90 min.

3. Propellant mass (use total Δv):

$$\frac{\Delta m}{m_0} = 1 - \exp\left(-\frac{\Delta v}{gI_{sp}}\right) = 0.5836 \quad (50)$$

Given $m_0 = 700 \text{ kg}$, $\Delta m = 408.5 \text{ kg}$ (quite high!)

It is not so obvious, but if you computed the propellant mass via a two-step procedure (i.e. the sum of Δm_1 due to Δv_1 and Δm_2 due to Δv_2), you would get the same result as above. In this approach take care to use the post-burn mass of the spacecraft after the first burn as the initial mass for the second burn.

10.1 Hohmann Transfer: Some Analysis

- Fig.(17) shows a plot of Δv 's involved in Hohmann transfer as a function of the ratio of radii, χ . The initial orbit is assumed to be circular at altitude 400 km. It is interesting to note that Δv_1 increases monotonically with χ , but eventually flattens out. From Eq.(39) it is easy to see that

$$\begin{aligned} \lim_{\chi \rightarrow \infty} \Delta v_1 &= \lim_{\chi \rightarrow \infty} v_i \left(\sqrt{\frac{2\chi}{\chi+1}} - 1 \right) \\ &= v_i(\sqrt{2} - 1) \\ &= \Delta v_{\text{escape}} !! \end{aligned} \quad (51)$$

which makes perfect sense! Can you explain why?

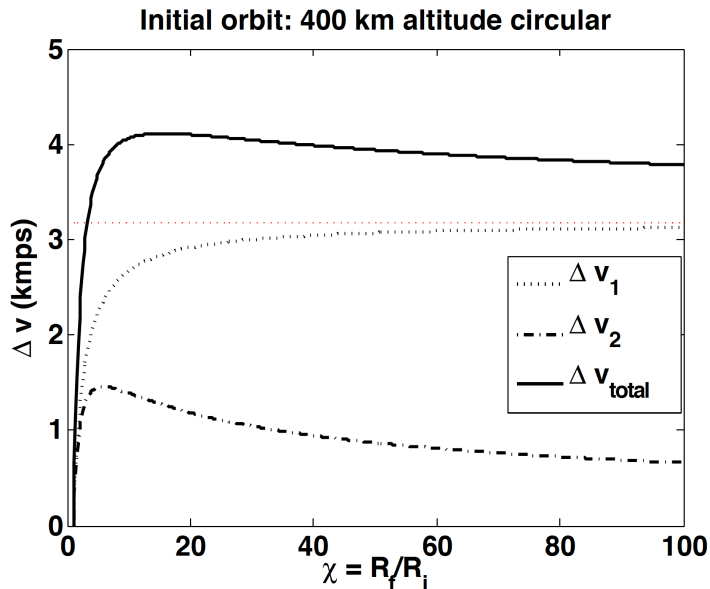


Figure 17: Hohmann transfer: Δv versus ratio of radii

Fig.(17) also shows that Δv_2 initially rises, then starts to decrease with χ . In fact,

$$\lim_{\chi \rightarrow \infty} \Delta v_2 = \lim_{\chi \rightarrow \infty} \frac{v_i}{\sqrt{\chi}} \left(1 - \sqrt{\frac{2}{\chi+1}} \right) = 0 !! \quad (52)$$

Combining Eqs.(51) and (52),

$$\lim_{\chi \rightarrow \infty} \Delta v_{\text{total}} = \lim_{\chi \rightarrow \infty} \Delta v_1 + \lim_{\chi \rightarrow \infty} \Delta v_2 = \Delta v_{\text{escape}} \quad (53)$$

- Next consider Fig.(18) that shows the transfer time as a function of χ . Clearly,

$$\lim_{\chi \rightarrow \infty} T = \infty \quad (54)$$

as expected.

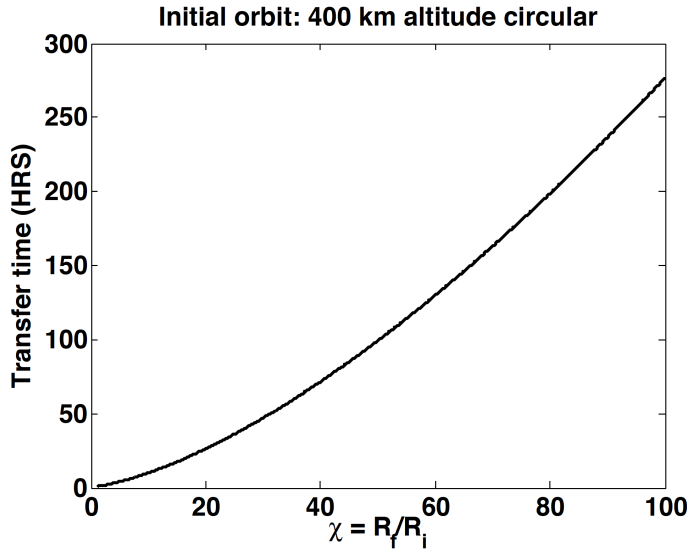


Figure 18: Hohmann transfer: Transfer time versus ratio of radii

- Fig.(19) is interesting and puts things in perspective. Δv 's for both the Hohmann transfer (solid line) and pure plane change (dashed line) are shown for the same initial orbit (circular @ 400 km altitude). On the x -axis the ratio $\Delta v/v_i$ is shown. The y -axis on the left shows χ , depicting the *reachable final orbit*, given a certain amount of Δv (read off the x -axis). The y -axis on the right shows Δi , depicting the achievable pure plane change.

Note that using the amount of Δv it takes to change the inclination by about 28 deg, the size of the initial orbit can be increased by about 95 times via a Hohmann transfer! Amazingly, it takes even less effort increase the orbit size even further (solid line moves to the left)!

11 Transfer to Geosynchronous Orbit

We will now study a real life application of the Hohmann transfer: delivering a spacecraft to a geostationary orbit. The objective is *to place a spacecraft in geostationary orbit starting from the Kennedy Space Center (KSC)*. There are many ways of doing this and we will consider three competing methods (in terms of Δv). In all methods, the first step is to launch the spacecraft into a so-called *parking orbit*.

- **Step I: Launch due East and injection into parking orbit.** The spacecraft begins its mission on the shown launch arc (solid red in Fig.(20)) originating from KSC (latitude = 28.6 deg). It is injected into a *parking orbit* (dotted green line marked O_1) at the shown location called the point of injection

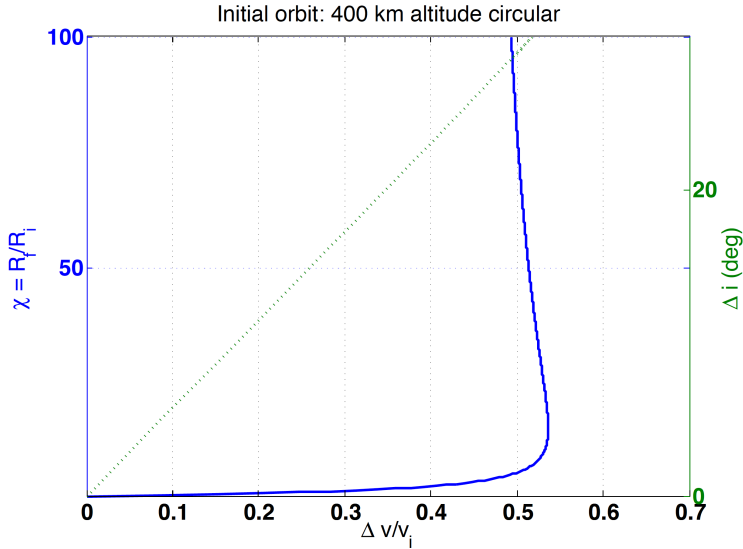


Figure 19: Hohmann transfer vis-a-vis pure plane change maneuver

(pink square). In the present analysis, we will not be concerned with the design of the launch arc. Effectively, our mission begins in the parking orbit. Typically, the parking orbit is circular @ 300 km altitude.

It is evident from Fig.(20) that the inclination of the parking orbit is related to the latitude of the launch site. In fact it depends on two things: (a) latitude of the launch site, ϕ (28.6 deg for KSC), and (b) the *azimuth angle* (Az) of spacecraft at the time of insertion into the parking orbit. Azimuth is the direction of the velocity vector at insertion. It is measured clockwise from the local meridian, such that “due North” is labeled 0 deg azimuth. As a result, an insertion made “due East” has an azimuth of 90 deg. Using spherical trigonometry, the inclination of the parking orbit can be shown to be

$$\cos i = \cos \phi \sin Az \quad (55)$$

When the insertion is made due East, $Az = 90$ deg, thus $i(O_1) = \phi(\text{KSC}) = 28.6$ deg. Keep in mind that our destination is the geostationary orbit, which is an equatorial circular orbit of radius $r_{\text{GEO}} = 42164$ km. Below, we will look at three methods of reaching this orbit.

11.1 Method A

This approach is illustrated in Fig.(21). Following injection into parking orbit (step I above), the spacecraft is transferred into an intermediate orbit, O_2 via a pure plane change. O_2 is equatorial and circular with the same radius as the parking orbit. Based on our discussion of plane changes, this maneuver must be performed at either the ascending node or descending node of the parking orbit. From the point of view of required effort, there is no difference between these two points (why?), thus the transfer to O_2 must be performed at the earliest available opportunity. Next, a Hohmann transfer is executed to arrive at the desired geostationary orbit (O_3 in Fig.(21)):

$$\text{Method A: } O_1 \xrightarrow{\Delta i (28.6^\circ)} O_2 \xrightarrow{\text{Hohmann}} O_3$$

Let us look at the Δv 's involved in this approach:

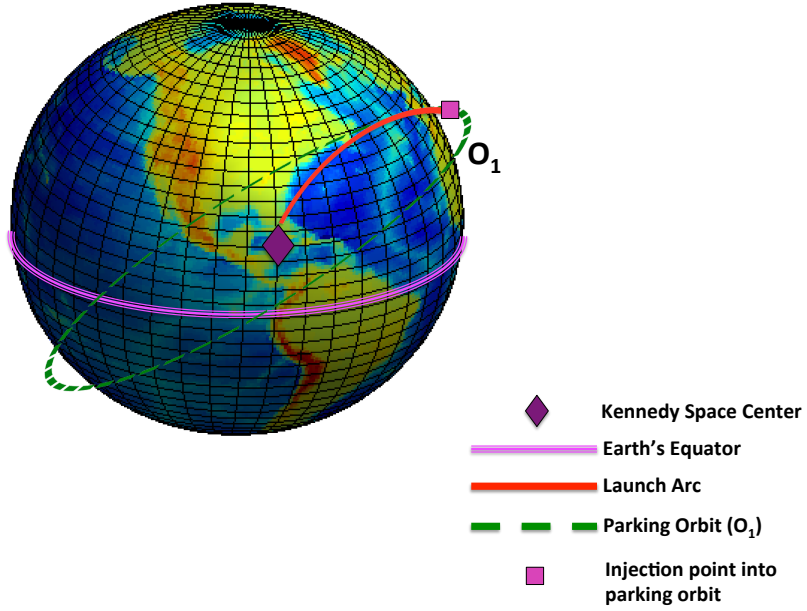


Figure 20: Injection into Parking Orbit from KSC

- **Step II(A): Plane change to O_2 .** For this maneuver, $v_i = v_{\text{park}}$

$$v_i = v_{O_1} = \sqrt{\frac{\mu}{r_{\text{park}}}} = \sqrt{\frac{\mu}{R_e + 300 \text{ km}}} = 7.7258 \text{ km/s} \quad (56)$$

The Δv needed to achieve the plane change therefore is

$$\Delta v_{A1} = 2v_i \sin \frac{\Delta i}{2} = 3.8165 \text{ km/s} \quad (\Delta i = 28.6 \text{ deg}) \quad (57)$$

- **Step III(A): Hohmann transfer to O_3 .** Note that following the plane change, O_2 and O_3 are co-planar so a Hohmann transfer works just fine. We do this step-by-step:

- **Step III(A).1: Transfer ellipse.** We have:

$$\begin{aligned} R_i &= r_{\text{park}} = R_e + 300 \text{ km} = 6678.14 \text{ km} \\ R_f &= r_{\text{geo}} = 42164 \text{ km} \end{aligned} \quad (58)$$

Thus $\chi = R_f/R_i = 6.3134$. Also,

$$a_t = \frac{R_i + R_f}{2} = 24,421 \text{ km} \quad (59)$$

$$P_t = 2\pi \sqrt{\frac{a_t^3}{\mu}} = 10.55 \text{ hrs} \quad (60)$$

- **Step III(A).2: Tangential Burns.** The following is the total Δv needed for the Hohmann transfer (both impulses):

$$\Delta v_{A2} = \underbrace{\Delta v_{A21}}_{1^{st} \text{ impulse}} + \underbrace{\Delta v_{A22}}_{2^{nd} \text{ impulse}} \quad (61)$$

For this maneuver, the initial velocity, $v_i = v_{O_2}$. We have:

$$\Delta v_{A2} = v_i \left[\sqrt{\frac{2\chi}{\chi+1}} - 1 + \frac{1}{\sqrt{\chi}} \left(1 - \sqrt{\frac{2}{\chi+1}} \right) \right] = 3.8926 \text{ km/s} \quad (62)$$

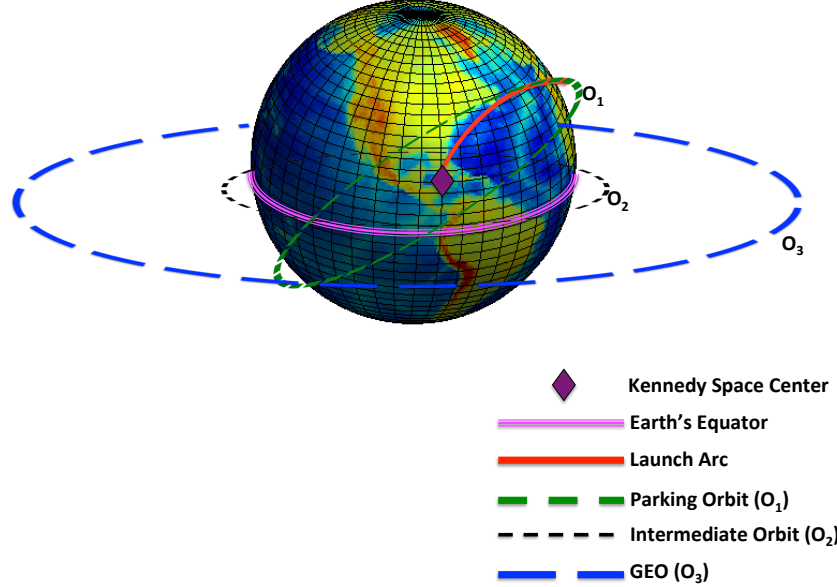


Figure 21: Transfer to Geostationary Orbit: Method A

Thus we get the total Δv needed:

$$\begin{aligned} \Delta v_{\text{Method A}} &= \underbrace{\Delta v_{A1}}_{\text{plane change: } O_1 \rightarrow O_2} + \underbrace{\Delta v_{A21} + \Delta v_{A22}}_{\text{Hohmann transfer: } O_2 \rightarrow O_3} \\ &= \boxed{7.7091 \text{ km/s}} \end{aligned} \quad (63)$$

The following is the total time needed for this mission:

$$\Delta T_{\text{Method A}} = \Delta T_{\text{PC wait}} + \Delta T_{\text{PC}} + \Delta T_{\text{Hoh. wait}} + \Delta T_{\text{Hoh.}} \quad (64)$$

where, $\Delta T_{\text{PC wait}}$ is the wait time before the initiation of the plane change maneuver. This depends on the distance of the point of injection from the ascending or descending node, whichever is closer. See Fig.(22): in this particular scenario, the injection point (IP, pink square) is closer to the descending node (DN). Since the parking orbit (O_1) is circular, whereby the time spent in an arc is proportional to the length of the arc (not true for elliptical orbits!), the time spent on the waiting arc (green) is

$$\Delta T_{\text{PC wait}} = \frac{(\pi - \theta_{ip})}{2\pi} P_{\text{park}} \quad (65)$$

For this example, let us assume that the “argument of injection”, $\theta_{ip} = 30$ deg. Thus $\Delta T_{\text{PC wait}} = (5/12)P_{\text{park}} = 0.63$ hr.

Next, ΔT_{PC} is the time needed for the plane change maneuver, which is zero since the plane change is a single impulse maneuver. $\Delta T_{\text{Hoh. wait}}$ is the wait time before the initiation of the Hohmann transfer and *also equals zero*. There is no need to wait after entering the intermediate orbit O_2 . Finally, $\Delta T_{\text{Hoh.}}$ is the time needed for execution of the Hohmann transfer, which equals $P_t/2 = 5.28$ hrs. Thus,

$$\Delta T_{\text{Method A}} = \Delta T_{\text{PC wait}} + \Delta T_{\text{Hoh.}} = (0.63 + 5.28) \text{ hr} = 5.9 \text{ hr} = 5 \text{ hr } 55 \text{ min} \quad (66)$$

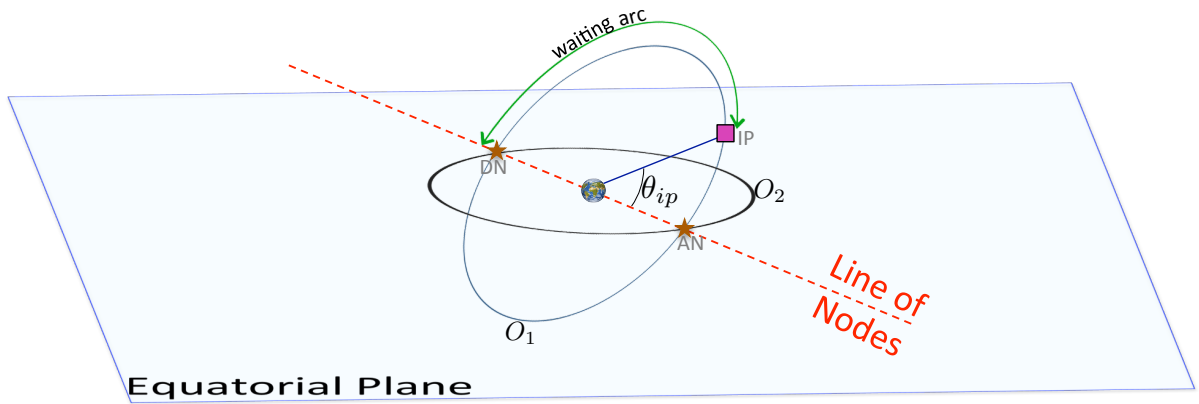


Figure 22: Waiting time for plane change: Method A

11.2 Method B

You must have realized working through method A that it is not the smartest way of transferring a spacecraft from its parking orbit to the geostationary orbit. The reason is simple: the plane change is conducted at the parking orbit where the speed is high. Why not wait until we reach the geostationary altitude before executing the plane change? We will refer to this approach as method B and it is illustrated in Fig.(23). The sequence of events goes as follows:

$$\text{Method B: } O_1 \xrightarrow{\text{Hohmann}} O'_2 \xrightarrow{\Delta i (28.6^\circ)} O_3$$

Here, after injection into the parking orbit, the spacecraft enters a Hohmann transfer between O_1 and an intermediate orbit O'_2 , which is circular, co-planar with the parking orbit and has an altitude equal to the geostationary altitude. Technically, the Hohmann maneuver can be initiated as soon as the injection into parking orbit is performed. Once in orbit O'_2 , the spacecraft must wait until it reaches the ascending (or descending) node to execute a plane change, thereby achieving the final desired equatorial geostationary orbit. We now examine the Δv 's involved in method B:

- **Step II(B): Hohmann transfer to O'_2 .** We have the following steps:

- **Step II(B).1: Transfer ellipse.** We have:

$$\begin{aligned} R_i &= r_{\text{park}} = R_e + 300\text{km} = 6678.14\text{km} \\ R_f &= r_{\text{geo}} = 42164\text{ km} \end{aligned} \tag{67}$$

Thus $\chi = R_f/R_i = 6.3134$. Also,

$$a_t = \frac{R_i + R_f}{2} = 24,421\text{ km} \tag{68}$$

$$P_t = 2\pi\sqrt{\frac{a_t^3}{\mu}} = 10.55\text{ hrs} \tag{69}$$

Interestingly, we see that the characteristics of the transfer ellipse are the same as in mission A. This is not really a surprise because the initial and final orbits are the same size as in method A. They just have a different inclination (both the initial and final orbits are co-planar at 28.6 deg).

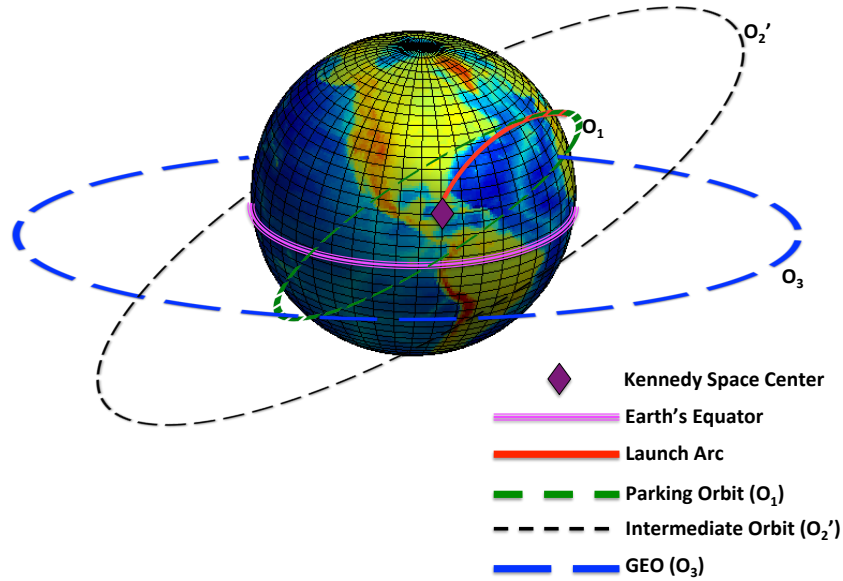


Figure 23: Transfer to Geostationary Orbit: Method B

- **Step II(B).2: Tangential Burns.** Since the initial and final orbits for this Hohmann maneuver have the same size as method A, the Δv 's involved will also be the same, and we have:

$$\Delta v_{B1} = \underbrace{\Delta v_{B11}}_{1^{st} \text{ burn}} + \underbrace{\Delta v_{B12}}_{2^{nd} \text{ burn}} \quad (70a)$$

$$= \Delta v_{A21} + \Delta v_{A22} \quad (\text{why?}) \quad (70b)$$

$$= 3.8926 \text{ km/s} \quad (70c)$$

- **Step III(B): Plane change from O_2' to O_3 .** Again looking at Fig.(23), we see that the final step is to reduce the inclination of the intermediate orbit (O_2') so it lies in the equatorial plane, coincident with the geostationary orbit. We must wait until the spacecraft arrives at the ascending or descending node of O_2' (whichever happens first) to execute this maneuver. The speed in orbit in O_2' is

$$v_{O_2'} = v_{\text{circular}}(r_{\text{geo}}) = \sqrt{\mu/r_{\text{geo}}} = 3.0747 \text{ km/s} \quad (71)$$

It is interesting to note that the above speed is less than half of the speed in the parking orbit (Eq.(56)). Since the Δv for plane change is directly proportional to the speed in orbit, we anticipate cutting the effort for plane change by more than half! To be more precise,

$$\Delta v_{B2} = 2v_{O_2'} \sin \frac{\Delta i}{2} = 1.5189 \text{ km/s} \quad (72)$$

Compare the above with Eq.(57).

Thus the total Δv for method B is:

$$\begin{aligned} \Delta v_{\text{Method B}} &= \underbrace{\Delta v_{B11} + \Delta v_{B12}}_{\text{Hohmann: } O_1 \rightarrow O_2'} + \underbrace{\Delta v_{B2}}_{\text{plane change: } O_2' \rightarrow O_3} \\ &= [5.4114] \text{ km/s} \end{aligned} \quad (73)$$

Compare the above with Eq.(63). Next we look at the time needed to execute mission B. The general form of Eq.(64) still holds:

$$\Delta T_{\text{Method B}} = \Delta T_{\text{Hoh. wait}} + \Delta T_{\text{Hoh.}} + \Delta T_{\text{PC wait}} + \Delta T_{\text{PC}} \quad (74)$$

where the terms in the RHS have the same meaning as in Eq.(64). Now, the way mission B has been described above, we enter the Hohmann transfer immediately following injection, whereby $\Delta T_{\text{Hoh. wait}} = 0$. Also, $\Delta T_{\text{Hoh.}} = P_t/2 = 5.28 \text{ hr}$. In order to determine the wait time for the plane change, we must figure out the point of arrival of the spacecraft in the intermediate orbit O'_2 . Fig.(24) shows the Hohmann transfer and the point of arrival at O'_2 (H : green circle). The spacecraft must therefore wait to arrive at the ascending node (AN) before the plane change maneuver can be performed. Thus the waiting arc between points H and AN is shown in green. Since the orbit O'_2 is circular, the time spent on this arc is proportional to the length of the arc, which is $(\pi - \theta_{ip})$. Therefore,

$$\Delta T_{\text{PC wait}} = \frac{(\pi - \theta_{ip})}{2\pi} P_{O'_2} \quad (75)$$

However, $P_{O'_2} = P_{O_3} = P_{\text{geo}}$, since the orbits O'_2 and O_3 are of the same size.

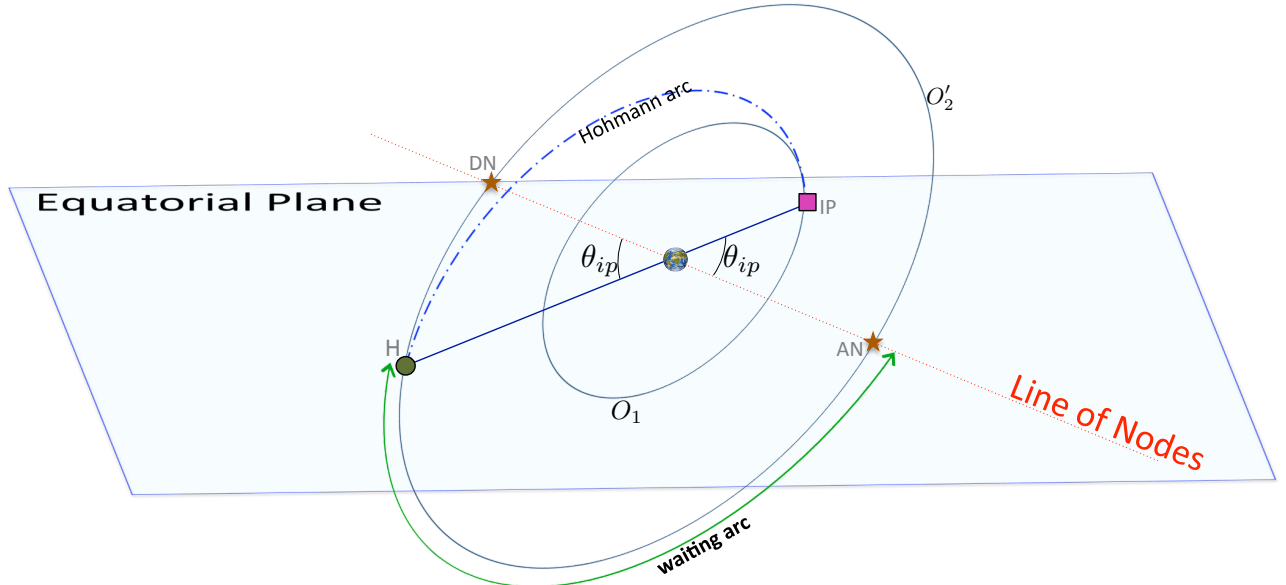


Figure 24: Waiting time for plane change: Method B

Of course, $\Delta T_{\text{PC}} = 0$, which gives us (assuming $\theta_{ip} = 30 \text{ deg}$):

$$\Delta T_{\text{Method B}} = \Delta T_{\text{Hoh.}} + \Delta T_{\text{PC wait}} = \frac{P_t}{2} + \frac{(\pi - \theta_{ip})}{2\pi} \underbrace{P_{\text{geo}}}_{24 \text{ hr}} = (5.28 + 10) \text{ hr} = 15 \text{ hr } 18 \text{ min} \quad (76)$$

Looking at Fig.(24), you may have noticed that there is a *faster* way to complete mission B. Clearly, the waiting time to reach the desired point for plane change is high because of the size of the orbit O'_2 . Can we therefore design the Hohmann transfer so that instead of terminating where it currently does (point H in Fig.(24)), it terminates at the ascending node of orbit O'_2 ? If yes, *the plane change can coincide with the arrival of the spacecraft at O'_2* and we would have $\Delta T_{\text{PC wait}} = 0$. This scenario is depicted in Fig.(25) and referred to as mission B*: note that it entails a wait period before the Hohmann transfer can be initiated; which is just fine because orbit O_1 is much smaller and “moves” much faster!

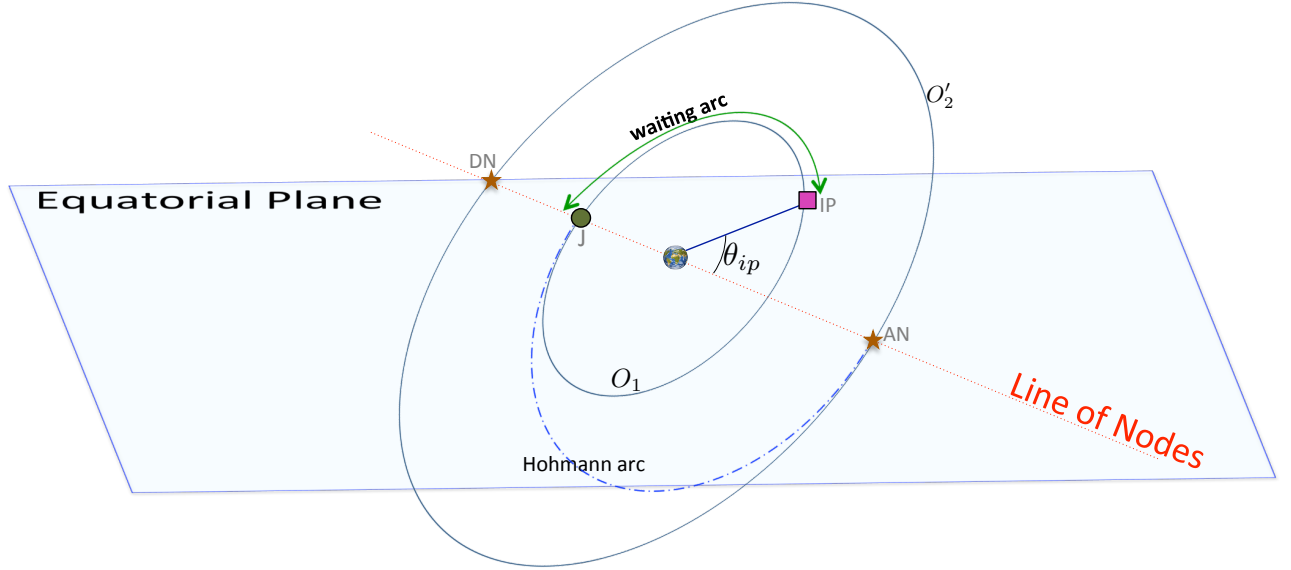


Figure 25: Waiting time for plane change: Method B*

From Fig.(25), the wait time for the Hohmann transfer is the time spent on the arc from the injection point (*IP*) to the descending node of the parking orbit (*J*). This arc measures $(\pi - \theta_{ip})$ and thus the wait time is:

$$\Delta T_{\text{Hoh. wait}} = \frac{(\pi - \theta_{ip})}{2\pi} P_{\text{park}} = 0.63 \text{ hr} \quad (77)$$

Thus for mission B* the total time of execution is:

$$\Delta T_{\text{Method B*}} = \Delta T_{\text{Hoh. wait}} + \Delta T_{\text{Hoh.}} + \Delta T_{\text{PC wait}} + \Delta T_{\text{PC}} \quad (78a)$$

$$= \frac{(\pi - \theta_{ip})}{2\pi} P_{\text{park}} + \frac{P_t}{2} + 0 + 0 \quad (78b)$$

$$= (0.63 + 5.28) \text{ hr} = 5 \text{ hr } 55 \text{ min} \quad (78c)$$

Of course, the total Δv for this mission (B*) remains the same as mission *B*, but mission B* takes much less time to execute than mission *B*, in fact, the same amount of time as mission A (compare Eq.(78c) and Eq.(76)).

11.3 A Composite Method

It is interesting to note that in the mission B* above, the burns Δv_{B12} and Δv_{B2} occur at the same place and the same time. They are performed sequentially, one after the other, at the point *AN* shown in Fig.(25). It turns out that we can *combine* these two burns into a single burn, resulting in further reduction of the overall Δv for the mission. As it currently stands, the two sequential burns executed at *AN* are shown in Fig.(26) below.

In Fig.(26), \mathbf{v}_{tA} is the velocity vector of the spacecraft on the Hohmann transfer ellipse at point *AN* in Fig.(25), and \mathbf{v}_{geo} is the velocity vector on the geostationary orbit, also at point *AN*. These three vectors are shown simultaneously in Fig.(27) below.

The “composite burn” is proposed in Fig.(28). The arrival velocity at *AN*, namely \mathbf{v}_{tA} is shown as *PQ* in Fig.(28). At the end of the first burn (Δv_{B2}), the velocity vector is $\mathbf{v}_{O'_2}$, shown as *PR* in Fig.(28). Finally, after the second burn at *AN* (Δv_{B2}) the velocity vector is \mathbf{v}_{geo} , shown by *PS*. Essentially, our the initial velocity vector is \mathbf{v}_{tA} and the *desired* final velocity vector is \mathbf{v}_{geo} . Instead of going from the former to the

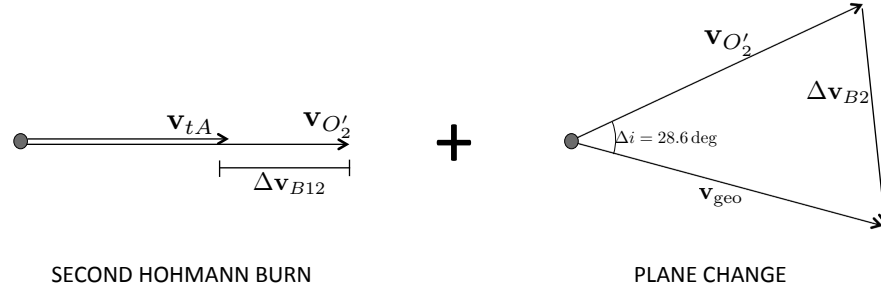


Figure 26: The sequence of two burns at AN in Method B^* , one immediately following the other.

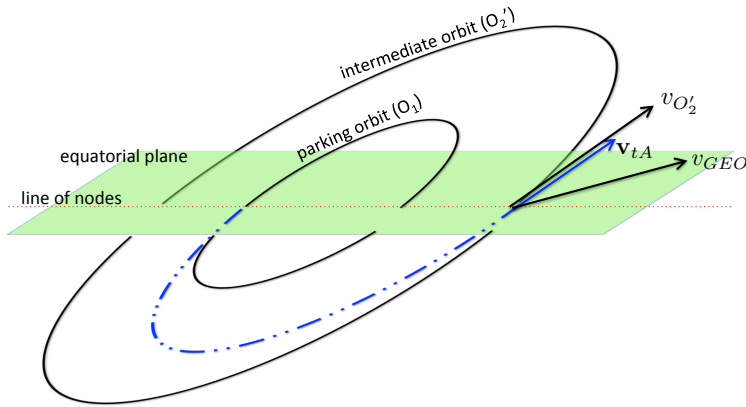


Figure 27: Geometry of the composite burn mission: B^*_{opt} (*optimized B^**).

latter via a two-step-process ($PQ - R - S$), the composite burn does so in a single shot. This is depicted by the burn Δv_C in Fig.(28), taking us through the direct route $PQ - S$.

By consideration of ΔQRS , it is trivial to show that the composite burn Δv_C is less than the two burn Δv_{B12} and Δv_{B2} combined. The proof comes simply from the triangle inequality, which states that the sum of any two sides of a triangle is always greater than the third side. Applied to ΔQRS we have

$$|QR| + |RS| > |QS| \quad (79)$$

Or,

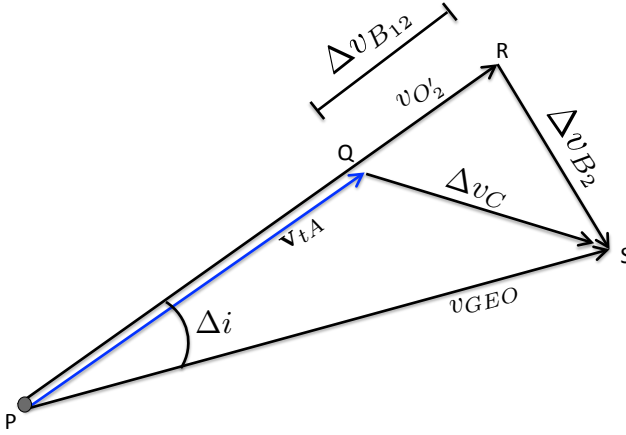
$$\Delta v_{B12} + \Delta v_{B2} > \Delta v_C \quad (80)$$

Having proved that the composite burn saves effort, all we need to do now is determine the magnitude of Δv_C . This is easy too: just solve the triangle PQS using the cosine-law:

$$\Delta v_C^2 = v_{tA}^2 + v_{\text{geo}}^2 - 2v_{tA}v_{\text{geo}} \cos \Delta i \quad (81)$$

Using known expressions from our notes on Hohmann transfer (in terms of χ),

$$\Delta v_C^2 = \frac{2v_i^2}{\chi(\chi+1)} + \frac{v_i^2}{\chi} - 2\sqrt{\frac{2}{\chi(\chi+1)}} \frac{v_i^2}{\sqrt{\chi}} \cos \Delta i \quad (82)$$

Figure 28: Geometry of the composite burn: mission B^*_{opt}

Or,

$$\boxed{\Delta v_C = \frac{v_i}{\sqrt{\chi}} \sqrt{\frac{\chi+3}{\chi+1} - \frac{2\sqrt{2}}{\sqrt{\chi+1}} \cos \Delta i}} \quad (83)$$

Substituting the numbers for our current application, we get

$$\boxed{\Delta v_C = 1.8325} \quad (84)$$

We refer to this “optimized version” of mission B^* as B^*_{opt} and see that the total Δv involved in this mission is:

$$\begin{aligned} \Delta v_{\text{Method } B^*_{\text{opt}}} &= \underbrace{\Delta v_{B11}}_{1^{st} \text{ Hohmann burn}} + \underbrace{\Delta v_C}_{\text{Composite Burn}} \\ &= (2.4257 + 1.8325) \text{ km/s} \\ &= \boxed{4.2582 \text{ km/s}} \end{aligned} \quad (85)$$

Clearly, mission B^*_{opt} is superior to both methods A and B^* . Moreover, it consumes the same time as method B^* :

$$\Delta T_{\text{Method } B^*_{\text{opt}}} = \Delta T_{\text{Hoh. wait}} + \Delta T_{\text{Hoh.}} + \Delta T_{\text{Comp wait}} + \Delta T_{\text{Comp}} \quad (86a)$$

$$= \frac{(\pi - \theta_{ip})}{2\pi} P_{\text{park}} + \frac{P_t}{2} + 0 + 0 \quad (86b)$$

$$= (0.63 + 5.28) \text{ hr} = 5 \text{ hr } 55 \text{ min} \quad (86c)$$

12 Multiple Impulse Maneuvers: Bielliptic Transfers

In Sec.(10), it was stated that the Hohmann transfer is the most fuel efficient two-impulse transfer possible between two coplanar circular orbits. If the number of impulses is increased to three, even better performance (i.e. lower Δv) is possible, but of course at the expense of even greater time-of-transfer than a Hohmann maneuver.

A *bielliptic transfer* employs two transfer ellipses and a total of three impulses; and under certain circumstances, provides better performance than a Hohmann transfer between the same initial and final orbits. Just as for the Hohmann maneuver, the initial and final orbits for a bielliptic transfer will be taken to be circular and coplanar.

- The motivation for a bielliptic transfer probably came from the performance of Hohmann transfers for very large final orbits. Recall that as χ (ratio of final to initial radii) becomes large, the second burn (Δv_2) in the Hohmann transfer decreases to zero.
- Fig.(29) shows the geometry of the bielliptic transfer. The initial orbit is O_i with radius R_i and the final orbit is O_f (radius R_f). The maneuver begins at point P , where a tangential burn transfers the spacecraft to the transfer ellipse TE_1 . TE_1 is much bigger in size than the final orbit O_f .

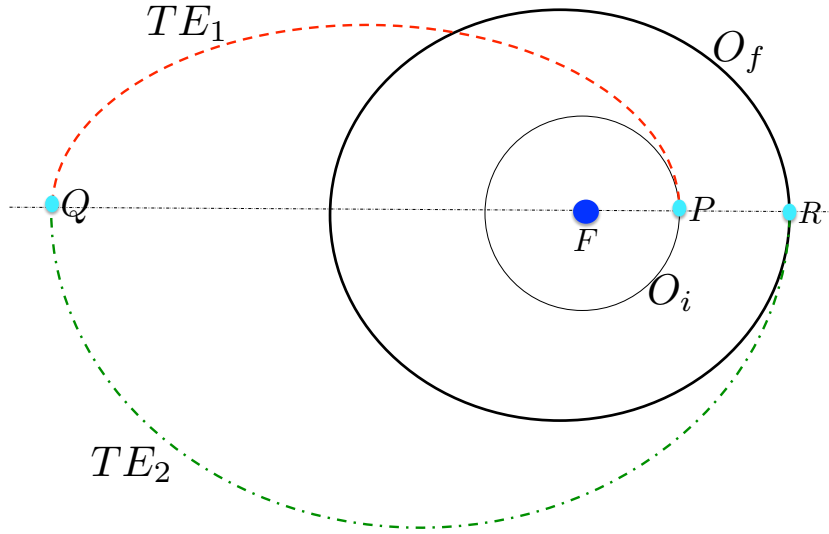


Figure 29: The Bielliptic Transfer between Coplanar Circular Orbits

After traversing half of TE_1 , another tangential burn (at Q) transfers the spacecraft into a second transfer ellipse, TE_2 which is designed to be tangential to the final orbit O_f at point R . When the spacecraft reaches R , it is moved from TE_2 to O_f using a third and final tangential burn.

- The first thing to note is that a bielliptic transfer is quite a leisurely maneuver (time-wise).
- The steps involved in the design of this maneuver are exactly the same as that for the Hohmann transfer, with the exception that here we have two transfer ellipses and three tangential burns as opposed to one ellipse and two burns in the former.
- Note that by construction, the point Q is the apoapsis of both transfer ellipses TE_1 and TE_2 . Let $FQ = R_a$ be the common radius of apoapsis. Then it is evident that:

$$a_1 = \frac{R_a + R_i}{2} \quad (87)$$

$$a_2 = \frac{R_a + R_f}{2} \quad (88)$$

where a_1 and a_2 are the semimajor axes of TE_1 and TE_2 respectively. Now, the speed on the initial and final orbits (O_i and O_f) are

$$v_i = \sqrt{\frac{\mu}{R_i}} \quad (89)$$

and

$$v_f = \sqrt{\frac{\mu}{R_f}} = \frac{v_i}{\sqrt{\chi}} \quad (90)$$

where χ is our familiar ratio

$$\chi \triangleq \frac{R_f}{R_i} \quad (91)$$

Let us define another ratio as follows

$$\beta \triangleq \frac{R_a}{R_i} \quad (92)$$

- Note that the radius of apoapsis, R_a is a *tuning parameter* in the bielliptic transfer. As a result, so is the ratio β . The ratio χ is not a tuning parameter: it has a fixed value and depends only on the initial and target orbits.
- By following the steps like in the Hohmann transfer, it is fairly straightforward to show that the total Δv for the bielliptic mission is given by

$$\Delta v_{BE} = \Delta v_P + \Delta v_Q + \Delta v_R \quad (93)$$

$$= v_i \left[\sqrt{\frac{2(\chi + \beta)}{\chi\beta}} - \frac{1 + \sqrt{\chi}}{\sqrt{\chi}} - (1 - \beta) \sqrt{\frac{2}{\beta(1 + \beta)}} \right] \quad (94)$$

- Let us look at what happens if we allow the transfer ellipses to grow in size. Consider the limit $\beta \rightarrow \infty$ and examine each one of the three burns individually:

$$\lim_{\beta \rightarrow \infty} \Delta v_P = \Delta v_{\text{escape},P} = v_i(\sqrt{2} - 1) \quad (95)$$

$$\lim_{\beta \rightarrow \infty} \Delta v_Q = 0 \quad (96)$$

$$\lim_{\beta \rightarrow \infty} \Delta v_R = \Delta v_{\text{escape},R} = v_f(\sqrt{2} - 1) \quad (97)$$

Keep in mind that as $\beta \rightarrow \infty$, both the transfer ellipses approach parabolas: TE_1 is the outgoing parabola and TE_2 is the incoming parabola. Therefore, Δv_Q must equal zero because the spacecraft is *essentially on the same (parabolic) orbit before and after the burn @ Q*.

Now, Δv_P must equal Δv_{escape} @ P because the spacecraft hops onto an escape parabolic orbit. The same is true for the point R , except that the transition is *from* the escape parabolic orbit onto the final desired orbit. The Δv for this transition is the same as that for the reverse (escape) maneuver. Combining Eqs.(95)-(97) into Eq.(93), we get

$$\lim_{\beta \rightarrow \infty} \Delta v_{BE} = v_i(\sqrt{2} - 1) + v_f(\sqrt{2} - 1) \quad (98)$$

But, $v_f = v_i/\chi$. Therefore,

$$\lim_{\beta \rightarrow \infty} \Delta v_{BE} = v_i \left[1 + \frac{1}{\sqrt{\chi}} \right] (\sqrt{2} - 1) \quad (99)$$

- The question is, when is $\Delta v_{BE} < \Delta v_{\text{Hohmann}}$? Fig.(30) answers this question comprehensively. On the x -axis is the ratio of the initial to final radii, i.e. χ . On the y -axis is the ratio of the TE apoapsis and the initial radius, β . Two boundaries are shown using solid black lines. The lower boundary (B_1) is the $\chi = \beta$ line and in the present comparison, we are only concerned with the area of the graph

above this boundary (below this boundary $R_a < R_i$ which is not relevant to bielliptic transfers). It is interesting also to note that along B_1 , the bielliptic transfer degenerates to the Hohmann transfer (both have identical geometries) and as a result, $\Delta v_{BE}/v_i = \Delta v_{\text{Hohmann}}/v_i$.

The second boundary (nonlinear curve B_2) was found as follows: (i) fix the value of χ , (ii) set $\Delta v_{BE}/v_i = \Delta v_{\text{Hohmann}}/v_i$ and find the value of β that satisfies this relationship, (iii) repeat for all values of χ . Essentially, the boundary B_2 is the locus of points along which the bielliptic and Hohmann transfers require the same amount of effort (equivalently, Δv , or fuel).

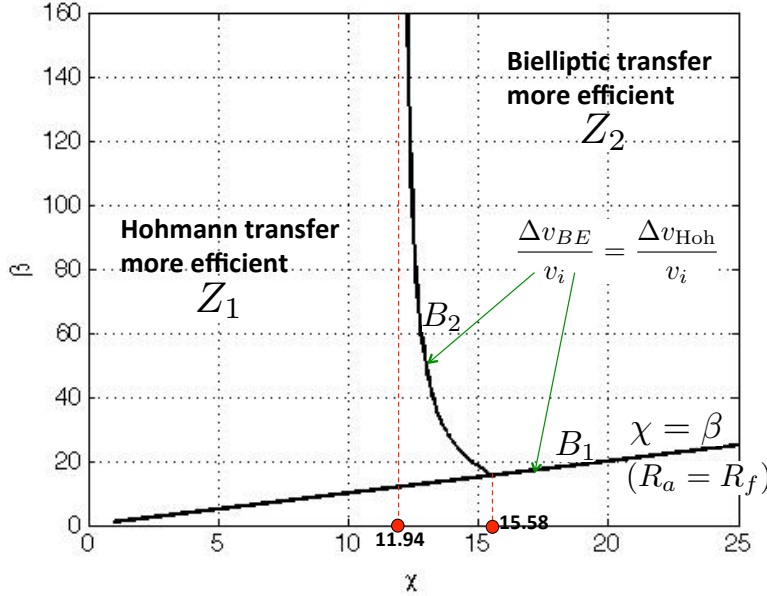


Figure 30: Comparative performance between the Hohmann and Bielliptic Maneuvers

- First of all, notice that there is only a small range of χ ($\in [11.94, 15.58]$) for which a β exists such that $\Delta v_{BE}/v_i = \Delta v_{\text{Hohmann}}/v_i$ along B_2 .
- The boundary B_2 divides the relevant region of the graph (the region above B_1) into two zones. The zone on the left (Z_1) is the region in which the Hohmann transfer is more fuel efficient than the bielliptic transfer. The zone on the right of B_2 , i.e. Z_2 is the region where the bielliptic transfer is more fuel efficient.
- Some examples:
 - i. Set $\chi = 10$. Except for the degenerate case of $\beta = \chi$, it is impossible to find a bielliptic transfer that outperforms the Hohmann transfer.
 - ii. Set $\chi = 13.25$, i.e. $R_f = 13.25R_i$. For this scenario, the bielliptic transfer burns the same amount of fuel as the Hohmann transfer if $\beta = 40$. For $13.25 < \beta < 40$, the bielliptic transfer is less efficient than the Hohmann transfer. However, for $\beta > 40$, the bielliptic transfer is more efficient. Of course, it will take much longer than the Hohmann transfer when $\beta > 40$.
 - iii. Finally, look at $\chi = 20$. Interestingly for all $\beta > 20$, the bielliptic transfer is more efficient than the Hohmann transfer.
- To summarize, Fig.(30) shows that for $\chi < 11.94$, the Hohmann transfer is always more efficient than the bielliptic transfer. Conversely, for $\chi > 15.58$, the bielliptic transfer is always more efficient than the Hohmann transfer. For $\chi \in [11.94, 15.58]$, the bielliptic transfer *can* be more efficient than the Hohmann transfer, provided it is “large enough” (more specifically, above the boundary B_2). Recall

that for the geostationary transfer $\chi \approx 7$. Therefore based on our analysis, it is not possible to design a bielliptic transfer that is better than the Hohmann transfer. Our numbers derived in the previous section are thus quite practical.

13 General Non-Hohmann Transfers

It was pointed out during the study of Hohmann maneuvers that they are somewhat slow. Sometimes, it is required to achieve a fast transfer (e.g. a rescue mission). In such instances, a transfer arc shorter than the one used in Hohmann transfers is utilized. See Fig.(31).

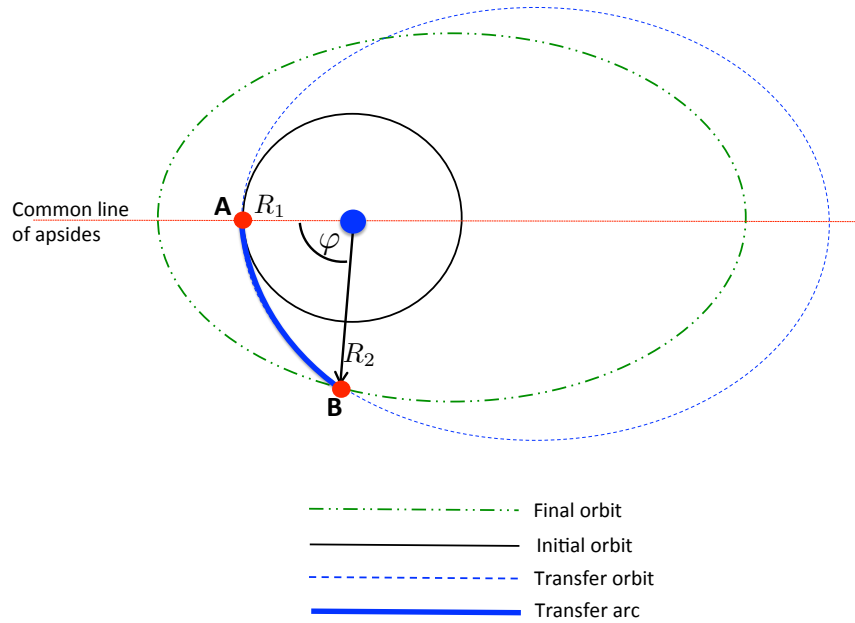


Figure 31: A non-Hohmann maneuver involving a short transfer arc

- To generalize our analysis just a little bit, we have allowed the final orbit to be elliptic (dashed green line) while the initial orbit is circular with radius R_1 .
- The transfer orbit is an ellipse that shares its line of apsides with the final orbit. *Please note that it doesn't have to be like that and this is a crucial simplifying assumption in our analysis.*
- The transfer arc (shown in solid blue) is the portion of the transfer ellipse that is actually traversed by the spacecraft. Since the line of apsides is shared, the point of intersection (point B) has the same true anomaly on the transfer ellipse and the final orbit (shown as φ).
- Clearly, the transfer arc is shorter than a Hohmann transfer. The benefit is a quicker transfer. The price to pay is greater Δv .
- It is apparent from Fig.(31) that the first burn is tangential, but the second burn is not.

Analysis of the non-Hohmann maneuver

- I. Design of the transfer ellipse.** By construction, the periapsis radius of the transfer ellipse equals the radius of the initial circular orbit,

$$r_{p_t} = R_1 = a_t(1 - e_t) = \frac{p_t}{1 + e_t} \quad (100)$$

where a_t , e_t and p_t are the semimajor axis, eccentricity and parameter of the transfer ellipse respectively (all unknown as this point). Let us now look at the point of the intersection between the transfer ellipse and the target orbit. As mentioned before, the true anomaly (φ) of this point is the same on both these orbit on account of the common line of apsides. In the present analysis, the transfer angle φ is treated as a tuning parameter. Note that when $\varphi = 180$ deg, we have the Hohmann transfer. The smaller φ is, the shorter the mission will be and we will tune it to control the characteristics of the transfer.

Let the radius of the intersection point be R_2 . From the equation of orbit applied to the transfer ellipse,

$$R_2 = \frac{p_t}{1 + e_t \cos \varphi} \quad (101)$$

We can also apply the equation of orbit to the target orbit,

$$R_2 = \frac{p_f}{1 + e_f \cos \varphi} \quad (102)$$

where, p_f and e_f are the parameter and eccentricity of the target orbit. If we fix the value of φ , R_2 is known. Thus we now have two equations (Eqs.(100), (102)) and two unknowns: (e_t, p_t) . These can be solved simultaneously to get

$$e_t = \frac{R_2 - R_1}{R_1 - R_2 \cos \varphi} \quad (103a)$$

$$p_t = R_1 R_2 \frac{1 - \cos \varphi}{R_1 - R_2 \cos \varphi} \quad (103b)$$

And of course, $a_t = r_{p_t}/(1 - e_t) = R_1/(1 - e_t)$.

- II. First Burn (@ A).** The first burn happens at the point A shown in Fig.(31) and is tangential. The initial speed is the speed on the circular orbit:

$$v_i = \sqrt{\frac{\mu}{R_1}} \quad (104)$$

Similarly, the speed @ A on the transfer ellipse is (from vis-viva):

$$v_{A_t} = \sqrt{\mu \left(\frac{2}{R_1} - \frac{1}{a_t} \right)} \quad (105)$$

Thus,

$$\Delta v_1 = \Delta v_A = v_{A_t} - v_i \quad (106a)$$

$$= \sqrt{\mu} \left[\sqrt{\frac{2}{R_1}} - \frac{1}{a_t} - \sqrt{\frac{1}{R_1}} \right] \quad (106b)$$

- III. Second Burn (@ B).** The second impulse occurs at the point B and is somewhat complex (since its not tangential). It involves both a magnitude change as well as a rotation of the velocity vector.

Let the velocity **vector** @ B on the transfer ellipse be \mathbf{v}_{t_B} and the velocity vector on the target orbit be \mathbf{v}_f . Thus we have

$$\Delta \mathbf{v}_B = \mathbf{v}_f - \mathbf{v}_{t_B} \quad (107)$$

We will express both the vectors on the RHS in the local $\hat{\mathbf{e}}_r - \hat{\mathbf{e}}_f$ frame. Recall that in general

$$\mathbf{v} = \dot{r}\hat{\mathbf{e}}_r + r\dot{f}\hat{\mathbf{e}}_f \quad (108)$$

where f is the true anomaly. Recall the following expressions for the \dot{r} and \dot{f} terms²:

$$\dot{r} = \sqrt{\frac{\mu}{p}} e \sin f; \quad \dot{f} = \frac{\sqrt{\mu p}}{r^2} \quad (109)$$

Thus Eq.(108) becomes

$$\mathbf{v} = \sqrt{\frac{\mu}{p}} e \sin f \hat{\mathbf{e}}_r + \frac{\sqrt{\mu p}}{r} \hat{\mathbf{e}}_f \quad (110)$$

Now, the question is, what about $\hat{\mathbf{e}}_r \times \hat{\mathbf{e}}_f$? We can express these in the orbital reference frame:

$$\hat{\mathbf{e}}_r = \cos f \hat{\mathbf{i}}_e + \sin f \hat{\mathbf{i}}_y \quad (111a)$$

$$\hat{\mathbf{e}}_f = -\sin f \hat{\mathbf{i}}_e + \cos f \hat{\mathbf{i}}_y \quad (111b)$$

This is especially good because the unit vectors $\hat{\mathbf{i}}_e$ and $\hat{\mathbf{i}}_y$ are the same for both the transfer and final orbits (remember they share their line of apsides). In fact, the true anomaly of point B is also the same on both the transfer ellipse and the final orbit: $f_{t_B} = f_{f_B} = \varphi$. We can write explicitly,

$$\hat{\mathbf{e}}_{r_{t_B}} = \cos \varphi \hat{\mathbf{i}}_e + \sin \varphi \hat{\mathbf{i}}_y = \hat{\mathbf{e}}_{r_{f_B}} \quad (112a)$$

$$\hat{\mathbf{e}}_{f_{t_B}} = -\sin \varphi \hat{\mathbf{i}}_e + \cos \varphi \hat{\mathbf{i}}_y = \hat{\mathbf{e}}_{f_{f_B}} \quad (112b)$$

Now, combining Eqs.(110) with (112), we have

$$\mathbf{v}_{f_B} = \underbrace{\sqrt{\frac{\mu}{p_f}} e_f \sin \varphi}_{\dot{r}} \underbrace{\left(\cos \varphi \hat{\mathbf{i}}_e + \sin \varphi \hat{\mathbf{i}}_y \right)}_{\hat{\mathbf{e}}_{r_{f_B}}} + \underbrace{\frac{\sqrt{\mu p_f}}{R_2}}_{r\dot{f}} \underbrace{\left(-\sin \varphi \hat{\mathbf{i}}_e + \cos \varphi \hat{\mathbf{i}}_y \right)}_{\hat{\mathbf{e}}_{f_{f_B}}} \quad (113)$$

Note that in the above equation, p_f and e_f are known, since they are parameters of the final (desired) orbit. Rearranging, Eq.(113),

$$\mathbf{v}_{f_B} = \left(\sqrt{\frac{\mu}{p_f}} e_f \sin \varphi \cos \varphi - \frac{\sqrt{\mu p_f}}{R_2} \sin \varphi \right) \hat{\mathbf{i}}_e + \left(\sqrt{\frac{\mu}{p_f}} e_f \sin^2 \varphi + \frac{\sqrt{\mu p_f}}{R_2} \cos \varphi \right) \hat{\mathbf{i}}_y \quad (114)$$

and by the same token,

$$\mathbf{v}_{t_B} = \left(\sqrt{\frac{\mu}{p_t}} e_t \sin \varphi \cos \varphi - \frac{\sqrt{\mu p_t}}{R_2} \sin \varphi \right) \hat{\mathbf{i}}_e + \left(\sqrt{\frac{\mu}{p_t}} e_t \sin^2 \varphi + \frac{\sqrt{\mu p_t}}{R_2} \cos \varphi \right) \hat{\mathbf{i}}_y \quad (115)$$

So that we can determine the required burn vector as given in Eq.(107). Now, the second burn can also be written, in significantly simpler terms, in the $(\hat{\mathbf{e}}_r, \hat{\mathbf{e}}_f)$ frame, which we already mentioned above, are identical for the transfer orbit and the final desired orbit:

$$\mathbf{v}_{f_B} = \sqrt{\frac{\mu}{p_f}} e_f \sin \varphi \hat{\mathbf{e}}_r + \frac{\sqrt{\mu p_f}}{R_2} \hat{\mathbf{e}}_f \quad (116a)$$

$$\mathbf{v}_{t_B} = \sqrt{\frac{\mu}{p_t}} e_t \sin \varphi \hat{\mathbf{e}}_r + \frac{\sqrt{\mu p_t}}{R_2} \hat{\mathbf{e}}_f \quad (116b)$$

such that

$$\Delta \mathbf{v}_B = \sqrt{\mu} \sin \varphi \left(\frac{e_f}{\sqrt{p_f}} - \frac{e_t}{\sqrt{p_t}} \right) \hat{\mathbf{e}}_r + \frac{\sqrt{\mu}}{R_2} (\sqrt{p_f} - \sqrt{p_t}) \hat{\mathbf{e}}_f \quad (117)$$

²These equations are easy to derive: simply look at $\mathbf{h} = \mathbf{r} \times \mathbf{v}$, such that $\mathbf{h} = r\hat{\mathbf{e}}_r \times (\dot{r}\hat{\mathbf{e}}_r + r\dot{f}\hat{\mathbf{e}}_f) = r^2\dot{f}$, whereby $\dot{f} = h/r^2 = \sqrt{\mu p}/r^2$. Also, differentiating the equation of orbit, $\dot{r} = p/(1+e \cos f)^2 e \sin f \dot{f} = \sqrt{\frac{\mu}{p}} e \sin f$

Recall that we can use the $\hat{\mathbf{e}}_r - \hat{\mathbf{e}}_f$ components of the velocity vector to determine the flight path angle ³:

$$\tan \gamma_{f_B} = \frac{\sqrt{\frac{\mu}{p_f}} e_f \sin \varphi}{\frac{\sqrt{\mu p_f}}{R_2}} = \frac{R_2}{p_f} e_f \sin \varphi \quad (118)$$

Similarly,

$$\tan \gamma_{t_B} = \frac{R_2}{p_t} e_t \sin \varphi \quad (119)$$

Thus the rotation angle for the velocity vector is nothing but

$$\Delta\gamma = \gamma_{f_B} - \gamma_{t_B} = \tan^{-1} \left(\frac{R_2}{p_f} e_f \sin \varphi \right) - \tan^{-1} \left(\frac{R_2}{p_t} e_t \sin \varphi \right) \quad (120)$$

Example Consider Fig.(32), which illustrates the non-Hohmann transfer between two circular orbits of altitude 300 km and 2000 km respectively. The transfer arc subtends an angle $\varphi = 90$ deg. We would like to compute the time saved over a traditional Hohmann transfer and the additional Δv needed.

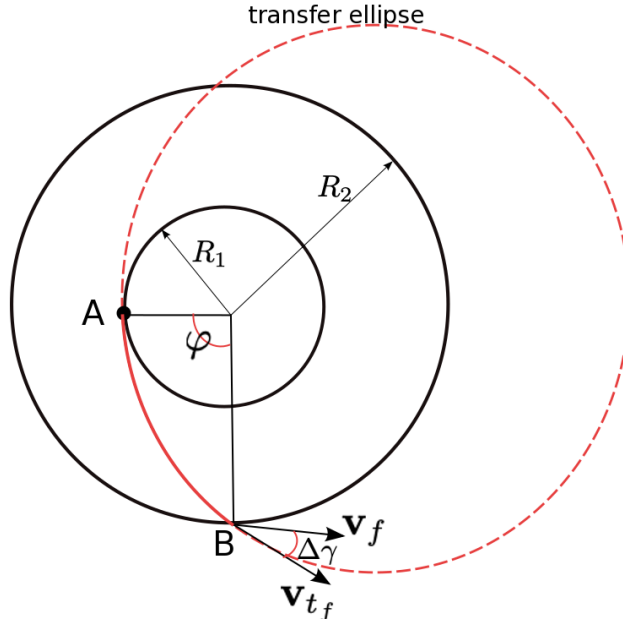


Figure 32: A Ninety-Degree Non-Hohmann Transfer

To begin, we consider the transfer ellipse:

- Eccentricity: Using Eq.(103a), we have

$$e_t = \frac{\chi - 1}{1 - \chi \cos 90^\circ} = 0.2546 \quad (121)$$

where of course, $\chi = R_2/R_1$ and in this case, $\chi = 1.2546$. Note that if $\chi = 2$, the transfer orbit for a 90° transfer arc is a parabola. Moreover, if $\chi > 2$, the transfer orbit (for $\varphi = 90^\circ$) is a hyperbola. Can you explain this?

³Recall: $\tan \gamma = \frac{v_{er}}{v_{ef}} = \frac{\dot{r}_f}{r_f}$

- Parameter p_t (Eq.(103b))

$$p_t = R_2 \frac{1 - \cos 90^\circ}{1 - \chi \cos 90^\circ} = R_2 = 8378.14 \text{ km} \quad (122)$$

- Semi-major axis: $a_t = p_t / (1 - e_t^2) = 8958.7 \text{ km}$.

Next, we consider the first burn, which is tangential:

$$v_i = \sqrt{\frac{\mu}{R_1}} = 7.7258 \text{ km/s} \quad (123)$$

$$v_{t_A} = \sqrt{\mu \left(\frac{2}{R_1} - \frac{1}{a_t} \right)} = 8.6534 \text{ km/s} \quad (124)$$

Thus, the first burn costs

$$\Delta v_1 = v_{t_A} - v_i = 927.65 \text{ m/s} \quad (125)$$

Use Eqs.(116) to compute the velocity vectors at point B on the transfer ellipse and desired orbits, respectively:

$$\begin{aligned} \mathbf{v}_{f_B} &= \sqrt{\frac{\mu}{p_f}} e_f \sin \varphi \hat{\mathbf{e}}_r + \frac{\sqrt{\mu p_f}}{R_2} \hat{\mathbf{e}}_f \\ &= [0, 6.8976] \text{ km/s} \end{aligned} \quad (126a)$$

$$\begin{aligned} \mathbf{v}_{t_B} &= \sqrt{\frac{\mu}{p_t}} e_t \sin \varphi \hat{\mathbf{e}}_r + \frac{\sqrt{\mu p_t}}{R_2} \hat{\mathbf{e}}_f \\ &= [1.7559, 6.8976] \text{ km/s} \end{aligned} \quad (126b)$$

To compute the second burn, we look at the difference between the two velocity vectors (recognize that we have a common reference frame), giving us

$$\begin{aligned} \Delta \mathbf{v}_B &= \mathbf{v}_{f_B} - \mathbf{v}_{t_B} \\ &= [-1.7559, 0] \text{ km/s} \end{aligned} \quad (127)$$

such that

$$\Delta v_B = \|\Delta \mathbf{v}_B\| = 1.7559 \text{ km/s} \quad (128)$$

We can look at the flight path angles to determine the rotation of the velocity vector:

$$\gamma_{f_B} = \tan^{-1} \left(\frac{R_2}{p_f} e_f \sin \varphi \right) = 0 \quad (129a)$$

$$\gamma_{t_B} = \tan^{-1} \left(\frac{R_2}{p_t} e_t \sin \varphi \right) = 14.3 \text{ deg} \quad (129b)$$

Thus

$$\Delta \theta = \gamma_{f_B} - \gamma_{t_B} = -14.3 \text{ deg} \quad (130)$$

The total effort for this non-Hohmann maneuver is

$$\Delta v_{\text{non-Hohmann}} = \Delta v_A + \Delta v_B = 2.6835 \text{ km/s} \quad (131)$$

And the travel time:

$$\Delta t_{\text{non-Hohmann}} = \frac{1}{n_t} (E_{B_t} - e \sin E_{B_t}) - \underbrace{(E_{A_t} - e \sin E_{A_t})}_{=0!} = 23.9 \text{ min} \quad (132)$$

where, of course,

$$E_{B_t} = 2 \tan^{-1} \left(\sqrt{\frac{1-e}{1+e}} \tan \frac{\phi}{2} \right) = 75.3 \text{ deg} \quad (133)$$

Let us compare this non-Hohmann mission with the Hohmann maneuver:

- Hohmann Transfer ellipse:

$$a_{t_H} = R_1(1+\chi)/2 = 7528.14 \text{ km} \quad (134a)$$

$$e_{t_H} = 0.11 \quad (134b)$$

$$P_{t_H} = 6500.4 \text{ s} = 1.8 \text{ hr} \quad (134c)$$

where, the H subscript is used for “Hohmann”.

- **Burns:** We use the Hohmann formula:

$$\Delta v_H = v_i \left[\sqrt{\frac{2\chi}{\chi+1}} - 1 + \frac{1}{\sqrt{\chi}} \left(1 - \sqrt{\frac{2}{\chi+1}} \right) \right] = 825.55 \text{ m/s} \quad (135)$$

which is significantly less than the non-Hohmann mission. The price to pay is the extra time:

$$\Delta t_H = P_{t_H}/2 = 54.2 \text{ min} \quad (136)$$

To finish off this example, let us sweep over the transfer angle, ϕ , recognizing that as $\phi \rightarrow \pi$, we must approach the Hohmann transfer numbers. This is shown in Figs.(33)

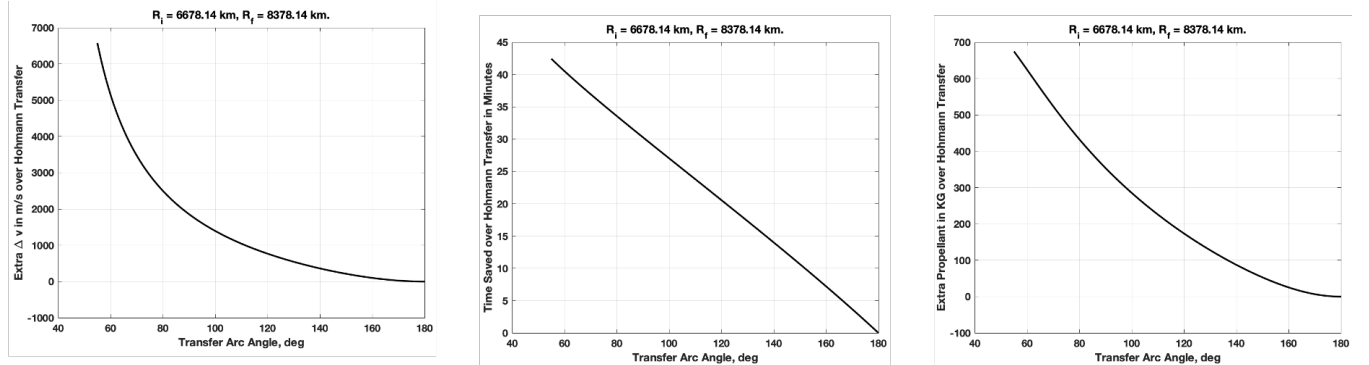


Figure 33: Non-Hohmann Transfer: Sweep Through Transfer Angle

14 Intercept Trajectories

In all maneuvers studied so far, the final burn ensures that the velocity of the spacecraft matches the velocity on the target orbit at the point of arrival. In other words, if there were a resident satellite on the final orbit present at the point and time of arrival, the transferred spacecraft would smoothly *rendezvous* the resident object (they would have zero relative velocity).

- There exists a class of maneuvers in which the final Δv is not performed. These are called intercept transfers. The objective in an intercept, is to simply “hit” the desired point of arrival in the final orbit at the desired time. If there is nothing else present to greet the incoming spacecraft at point B in Fig.(34), it will simply shoot past the target orbit, continuing its path of the transfer orbit. If however, if something is present at the point and time of arrival, the transferred spacecraft will collide with the resident object with non-zero relative velocity, completing the “intercept” maneuver.

- In a nutshell, the burn Δv_B is not performed in an intercept maneuver. The following is the difference between rendezvous and intercept:

- **Intercept:** match only position vectors (\mathbf{r}), i.e., simply "hit a point".
- **Rendezvous:** match both position and velocity vectors (\mathbf{r}, \mathbf{v}), such that we meet the target orbit "smoothly".

Clearly, the difference between the two is that in the former, the final Δv is not performed.

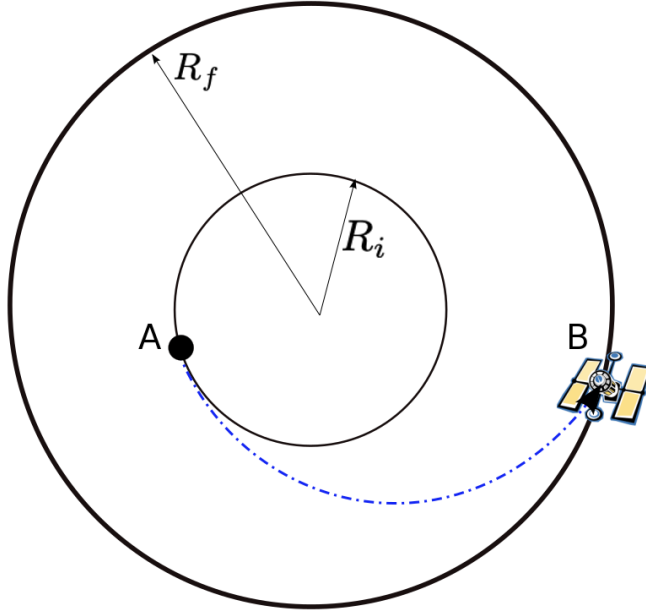


Figure 34: An intercept trajectory between two circular orbits: same as a “normal transfer”, except that we do not perform the final burn.

15 Phasing Maneuvers

We will consider the following version of the so-called phasing problem: two spacecraft S_1 and S_2 are initially stationed in a common circular orbit, O_i , as shown in Fig.(35), and separated by phase angle β . Due to the nature of the orbit, the phase angle is time invariant. The objective of the phasing maneuver is for spacecraft S_1 to rendezvous with spacecraft S_2 .

- Without loss of generality, we stipulate the point of rendezvous to be point A . The approach will be to transfer S_1 to a higher orbit (dotted transfer orbit, O_t), and simply wait. The transfer orbit O_t is designed such that after a few go-arounds, both S_1 and S_2 will meet at point A . At this moment, S_1 is transferred back to O_i , thus completing the rendezvous.
- Let us begin our analysis with the following observations and definitions:
 - Radius of home orbit O_i : R .
 - Speed on O_i : $v_i = \sqrt{\frac{\mu}{R}}$.
 - Period of transfer orbit: P_t : this is to be determined.

- Let S_1 complete k full orbits on O_t before rendezvous occurs at A .
- Clearly, the total wait time for rendezvous is

$$T_{\text{wait}} = kP_t \quad (137)$$

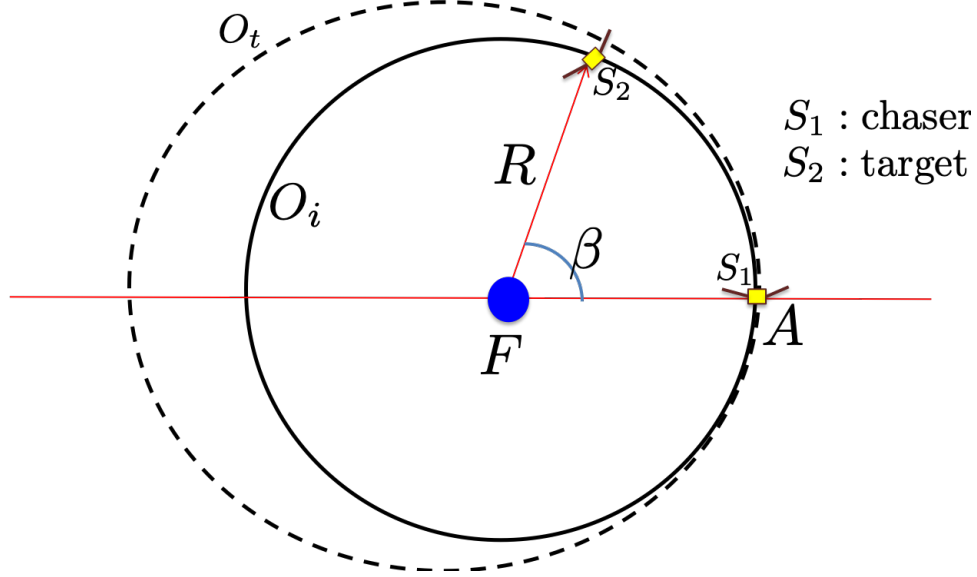


Figure 35: The set up for a phasing maneuver on a circular orbit.

- During the above time, the target spacecraft S_2 covers the following angle:

$$\varphi_{S_2} = \underbrace{(2\pi - \beta)}_{\text{lead angle}} + \underbrace{2\pi q}_{\text{additional } 'q' \text{ orbits}} \quad (138)$$

Alternatively, note that the angular speed of S_2 is $n_i = 2\pi/P_i$. Since the wait time (Eq.(137)) is the time of traversal for S_2 , the total “angular distance” covered by S_2 is

$$\begin{aligned} \text{angular distance} &= \text{angular speed} \times \text{time} \\ &= n_i k P_t \end{aligned} \quad (139)$$

Comparing Eqs.(138) and (139), we get

$$\varphi_{S_2} = (2\pi - \beta) + 2\pi q = n_i k P_t \quad (140)$$

giving us that

$$P_t = \frac{2\pi(q+1) - \beta}{kn_i} \quad (141)$$

where, q and k are design variables and must be decided by the user.

- Note that k and q in Eq.(141) are not arbitrary. In fact, they are both integers and $k_{\min} = 1$. From Eq.(140),

$$\begin{aligned} \text{RHS} &= kn_i P_t = k \frac{2\pi}{P_i} P_t > 2\pi k \\ \text{I.E., } kn_i P_t &> 2\pi k \end{aligned} \quad (142)$$

since $P_t > P_i$. Use Eq.(142) in Eq.(140),

$$q > \left(k - 1 + \frac{\beta}{2\pi} \right) \quad (143)$$

Given that q must be an integer, we land with

$$q_{\min} = k \quad (144)$$

- So, here's the strategy:

- Pick k .
- Then, pick q , such that $q_{\min} = k$. Determine P_t , given by Eq.(141).

- A special case arises when $q = q_{\min} = k$. We have

$$\begin{aligned} P_t^* &\stackrel{\text{Eq.(141)}}{=} \frac{2\pi(k+1) - \beta}{kn_i} \\ &= \frac{2\pi}{n_i} + \frac{2\pi - \beta}{kn_i} \\ &= P_i + \frac{2\pi - \beta}{kn_i} \end{aligned} \quad (145)$$

- Computation of Δv : There are two burns: Δv_1 and Δv_2 , both occurring at A :

- Δv_1 transfers the chaser S_1 from O_i to O_t , at A .
- Δv_2 transfers chaser S_1 from O_t to O_i , at A , completing the rendezvous.

The two burns are mirror images of each other and therefore must be equal in magnitude: $|\Delta v_1| = |\Delta v_2|$. Moreover, each burn is tangential, such that

$$\Delta v_1 = v_{A_t} - v_i \quad (146)$$

where, v_{A_t} is the speed on O_t at A , given below (vis viva):

$$v_{A_t} = \sqrt{\frac{2\mu}{R} - \frac{\mu}{a_t}} \quad (147)$$

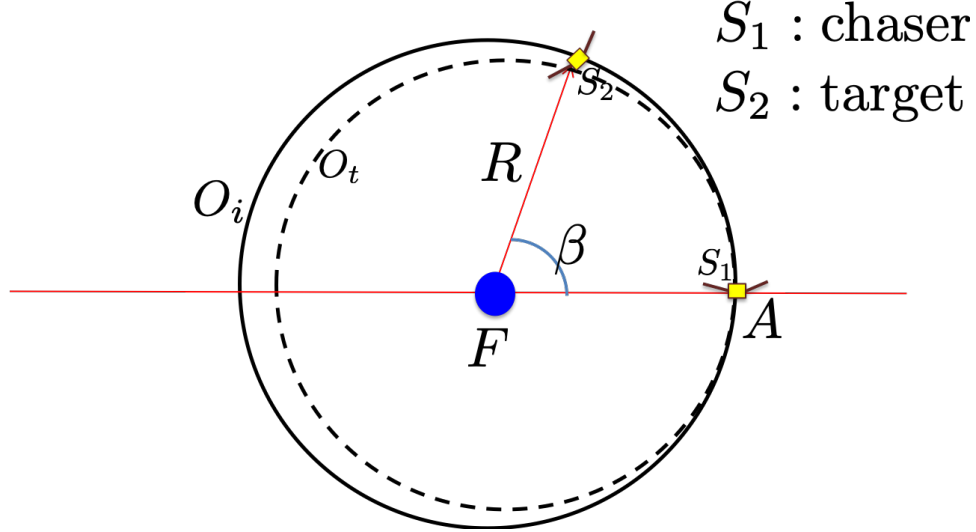
where,

$$a_t = \left(\frac{\mu P_t^2}{4\pi^2} \right)^{1/3} \quad (\text{Kepler's Third}) \quad (148)$$

Thus, we get (using P_t from Eq.(141)):

$$\Delta v = \Delta v_1 + \Delta v_2 = 2 \left(\sqrt{\frac{2\mu}{R} - \frac{\mu}{a_t}} - \sqrt{\frac{\mu}{R}} \right) \quad (149)$$

- Now, in the above analysis, S_1 is the chaser while S_2 , the leading spacecraft is the target. We say that S_2 leads S_1 by phase β . Equivalently, S_1 lags S_2 by phase β .
- It makes sense to inquire whether a lagging chaser can rendezvous by transferring to a “lower orbit” instead of a higher orbit and waiting out the phase closure: see Fig.(36). The transfer ellipse O_t is now such that its apoapsis radius equals R : $r_a = R$.
- The analysis for this maneuver mirrors the one for the higher transfer:
 - Let S_1 wait out k orbits on O_t , such that its total wait time is kP_t .

Figure 36: Phasing through transfer to a *lower orbit*.

- During this time, S_2 covers the following angular distance: $(2\pi - \beta) + 2\pi q$, where q is the number of full orbits covered by S_2 prior to rendezvous.
- As for the higher orbit transfer case, we get

$$P_t = \frac{2\pi(q+1) - \beta}{kn_i}$$

In this case however, $P_t < P_i$, giving us

$$kP_t n_i = 2\pi k \frac{P_t}{P_i} < 2\pi k \quad (150)$$

Thus

$$\begin{aligned} (2\pi - \beta) + 2q\pi &= kP_t n_i < 2\pi k \\ \Rightarrow q &< k - 1 + \frac{\beta}{2\pi} \end{aligned} \quad (151)$$

Or, $q_{\max} = k - 1$, since k and q are integers and $0 < \beta/2\pi < 1$.

In the special case that $q = q_{\max} = k - 1$ to get that

$$P_t = \frac{2\pi}{n_i} - \frac{\beta}{kn_i}$$

Or,

$$P_t = P_i - \frac{\beta}{kn_i} \quad (152)$$

Finally, the Δv computation is similar: now the point A is the apoapsis of O_t :

$$v_{A_t} = \sqrt{\frac{2\mu}{R} - \frac{\mu}{a_t}}$$

where, $a_t = (\mu P_t^2 / 4\pi^2)^{1/3}$. As before, we get

$$\Delta v = \Delta v_1 + \Delta v_2 = 2 \left(\sqrt{\frac{\mu}{R}} - \sqrt{\frac{2\mu}{R} - \frac{\mu}{a_t}} \right) \quad (153)$$

Example Consider a lagging chaser S_1 trailing the target S_2 by $\beta = 20 \text{ deg}$ in a circular home orbit of altitude 300 km, as shown in Fig.(37). Determine the minimum Δv phasing maneuver that achieves rendezvous of S_1 with S_2 at point A within 10 hours.

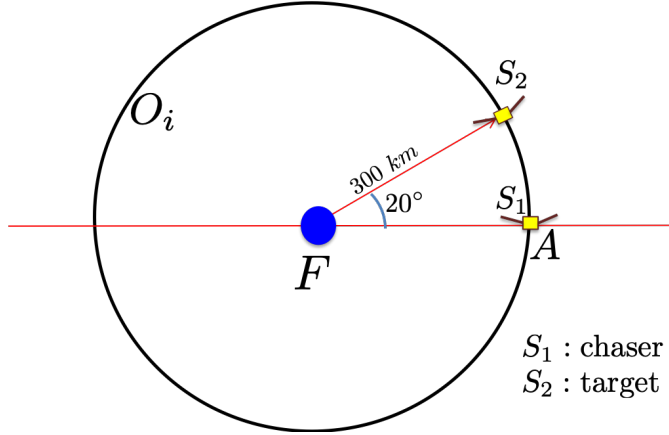


Figure 37: Phasing maneuver example: lagging chaser

Solution. We have $P_i = 2\pi\sqrt{R^3/\mu} = 1.51 \text{ hr}$. There are four categories of phasing maneuvers in all:

- I. Transfer to high transfer orbit: here, point A is the periapsis of the transfer orbit. We have two subcases:
 - a.) $q = q_{\min} = k$. In this case, the period of the transfer orbit is given by Eq.(145), as a function of k .
 - b.) $q > k$. The period of the transfer orbit is given by the general equation stated in Eq.(141).

- II. Transfer to lower transfer orbit: here, point A is the apoapsis of the transfer orbit. We have two subcases:

- a.) $q = q_{\max} = k - 1$. In this case, the period of the transfer orbit is given by Eq.(152), as a function of k .
- b.) $q < k - 1$. The period of the transfer orbit is given by the general equation stated in Eq.(141).

Remember that k is the number of complete orbits covered by the chaser S_1 in its transfer orbit. A variation of P_t -versus- k for cases I.a) and II.a) is shown in Fig.(38). In this plot k is varied from one to ten. It is interesting to note that the period of the transfer orbit (hence its size) is closer to the home orbit (O_i) for a lower transfer-orbit. This indicates that the transfer orbit O_t is more similar to the home orbit O_i when a “lower transfer” is employed such that a small effort may be needed to achieve the rendezvous via the lower phasing maneuver. We will see if this is true.

It is also visible that in both cases I.a) and II.a), the transfer orbit period is closer to the home orbit period for larger values of k . This makes intuitive sense. Note that the idea behind transferring the chaser to O_t is to create a phase-rate between itself and the target. The objective is to close out the phase deficit, β . By allowing to increase the value of k , we are willing to wait longer to close out the phase deficit, which in turn implies a smaller phase-rate is acceptable. In other words, a larger k implies a smaller difference between the orbits O_i and O_t and as a result, P_i and P_t .

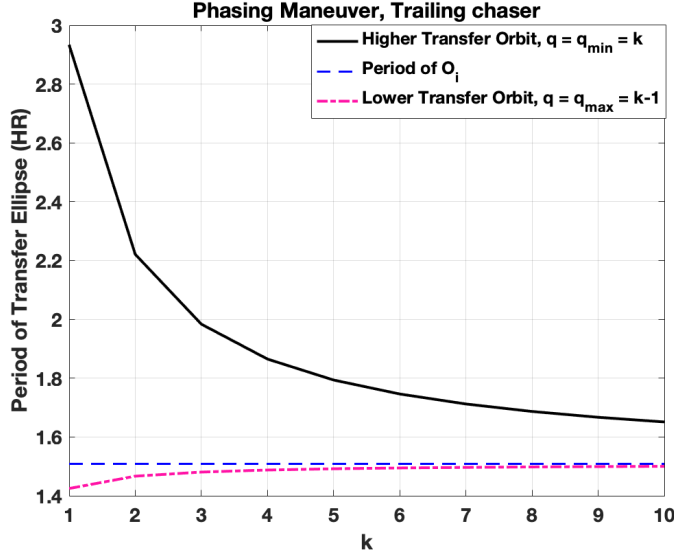


Figure 38: Phasing maneuver example: Period of Transfer Orbit: Cases I.a) and II.a)

Now, note that a limit has placed on the total time allowed for the maneuver (10 hrs). This is plotted in Fig.(39) for cases I.a) and II.a). For the higher transfer-orbit case, the largest possible value for k is $k_{\max} = 5$. For the lower transfer-orbit case, the largest possible value is $k_{\max} = 6$. Beyond these values of k , the total mission time exceeds the specified cut-off of 10 hours (shown in dashed-blue).

Finally, Fig.(40) shows the total mission Δv required for cases I.a) and II.a) (Eqs.(149) and (153) respectively). Clearly, in both cases, $\Delta v \downarrow$ as $k \uparrow$. This plot supports the intuitive arguments given above that the transfer orbit characteristics are closer to the home orbit characteristics for a larger k . Consequently, less effort is required to transfer to- and from- O_t . In other words, $k \uparrow \Rightarrow \Delta v \downarrow$.

It is less intuitive as to why a lower transfer-orbit achieves more efficient phasing than a higher transfer-orbit. This has to do with the relative placement of the chaser with respect to the target, vis-à-vis the net effect of each transfer. Note that by transferring the chaser to a lower orbit, we are effectively speeding it up with respect to the target. Since the chaser is trailing the target by a small angle, this appears to be the logical choice. On the other hand, by transferring the chaser to a higher transfer orbit, we are slowing it down with respect to the home orbit. This will cause its lag to increase further, eventually causing the lag to increase to a full orbit, at which point the maneuver is complete. Clearly, this appears to be less effective for a lag of less than half an orbit, i.e. $\beta < \pi$. Try out the code attached in Carmen to see if the higher transfer-orbit becomes preferable over the lower transfer-orbit when $\beta > \pi$.

To round off this part, let us compute the numbers corresponding to the more efficient maneuver possible in each case:

- Case I.a): $k_{\max} = 5$. $P_t(k = 5, q = q_{\min} = k) = 1.79$ hr. Resulting $\Delta v(k = 5, q = q_{\min} = k) = 0.82$ km/s and time needed for maneuver: $T_{\text{wait}}(k = 5, q = q_{\min} = k) = kP_t = 8.97$ hr.
- Case II.a): $k_{\max} = 6$. $P_t(k = 6, q = q_{\max} = k-1) = 1.49$ hr. Resulting $\Delta v(k = 6, q = q_{\max} = 5) = 0.05$ km/s and time needed for maneuver: $T_{\text{wait}}(k = 6, q = q_{\max} = k-1) = kP_t = 8.96$ hr.

Clearly, Case II.a) is far superior than Case I.a).

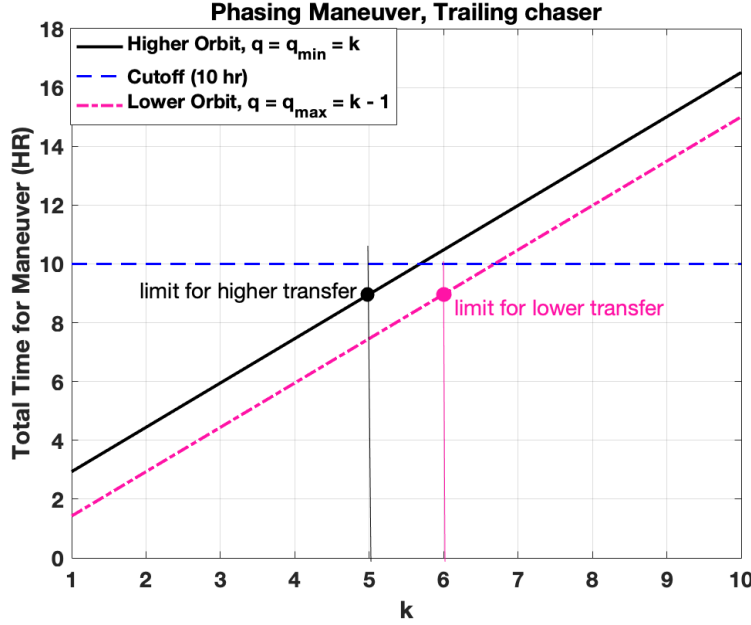


Figure 39: Phasing maneuver example: Time to Transfer: Cases I.a) and II.a)

In the next leg of analysis, let us consider the case when $q > k$ for a higher transfer-orbit and $q < k - 1$ for a lower transfer-orbit. In both these cases, we will vary q , while setting k to be at its largest possible numerical value (as argued and demonstrated above, a larger k is more efficient, irrespective of direction of transfer). Thus for Case I.b), we set $k = 5$ and for Case II.b), set $k = 6$. In the former, vary q as $q > k$ and in the latter as $q < k - 1$. Fig.(41) shows the variation of transfer-orbit period with respect for q . Note that we cannot allow the transfer orbit period to be arbitrarily small because at some point, its periapsis would lie within the surface of Earth. A light-blue line shows the period of an orbit with semi-major axis equal to the radius of Earth. This is an absolute cutoff because it guarantees a periapsis within the Earth's surface ($r_p < a$). By this argument, $q < k - 1$ is not possible and Case II.b) is ruled out. Case I.b) is still possible with $q > k = 5$ (solid black line).

Fig.(42) shows the total maneuver times for Cases I.b) and II.b). This figure rules out Case I.b) as well because $T_{\text{wait, upper}}(q > 5) > 10 \text{ hr}$. In any case, neither of these cases are any better in terms of mission Δv because of the “greater distance” between the home orbit and transfer orbit: see Fig.(43). For Case I.b), $\Delta v(q > k) > \Delta v(q = k)$ for all. Similarly, for Case II.b), $\Delta v(q < k - 1) > \Delta v(q = k - 1)$. Thus, there isn’t much benefit in exploring the phasing maneuvers beyond Cases I.a) and II.a).

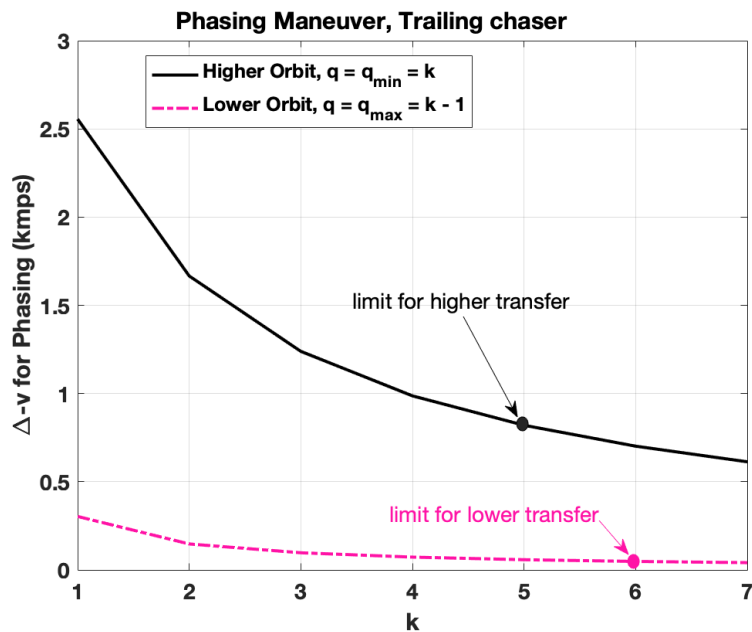
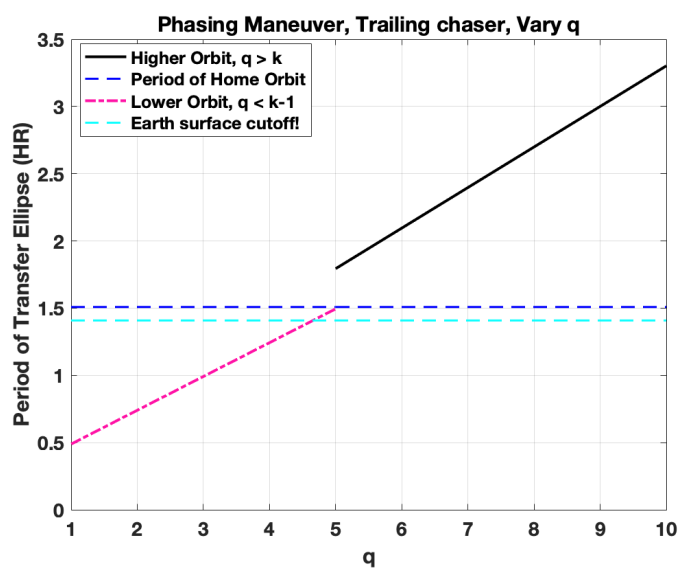
Figure 40: Phasing maneuver example: Mission Δv : Cases I.a) and II.a)

Figure 41: Phasing maneuver example: Period of Transfer Orbit: Cases I.b) and II.b)

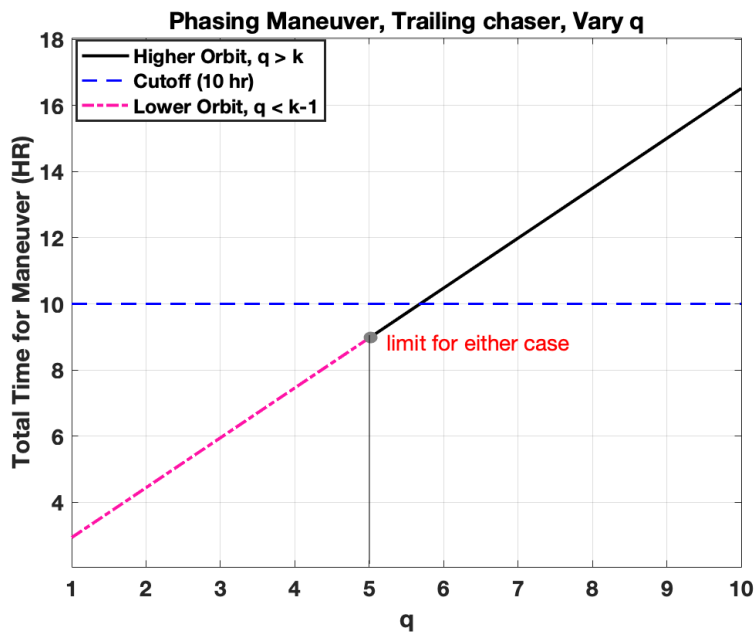
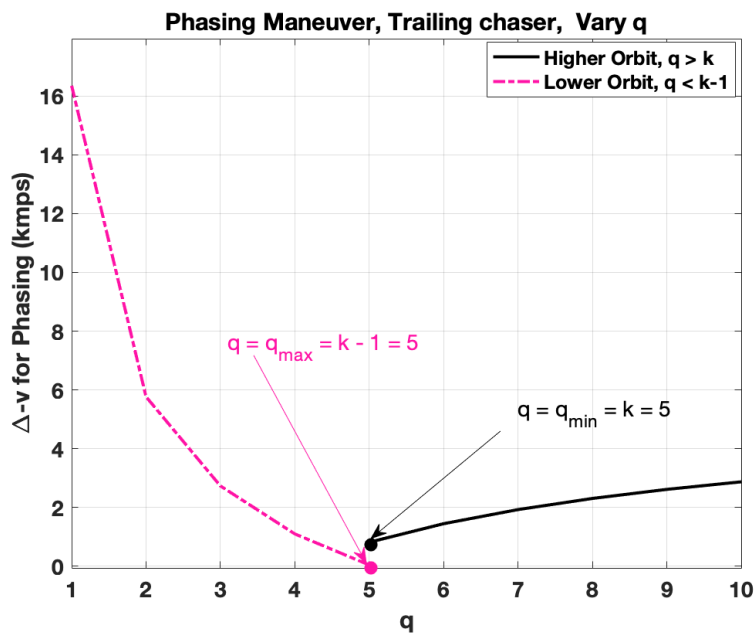


Figure 42: Phasing maneuver example: Time to Transfer: Cases I.b) and II.b)

Figure 43: Phasing maneuver example: Mission Δv : Cases I.b) and II.b)